ANKARA YILDIRIM BEYAZIT UNIVERSITY
GRADUATE SCHOOL OF NATURAL AND APPLIED SCIENCES

EXPERIMENTAL STUDY OF BRILLOUIN FREQUENCY SHIFT ON CLASSICAL AND MODERN BOTDA, BOTDR SETUPS

M.Sc. Thesis by
Abdullah Erkam GÜNDÜZ

Department of Electronics and Communication Engineering

November, 2016

ANKARA

EXPERIMENTAL STUDY OF BRILLOUIN FREQUENCY SHIFT ON CLASSICAL AND MODERN BOTDA, BOTDR SETUPS

A Thesis Submitted to the

Graduate School of Natural and Applied Sciences of AnkaraYıldırım Beyazıt University

In Partial Fulfillment of the Requirements for the Master of Science in

Electronics and Communication Engineering, Department of Electronics and Communication Engineering

by

Abdullah Erkam GÜNDÜZ

November, 2016

ANKARA

M.Sc THESIS EXAMINATION RESULT FORM

We have read the thesis entitle **''Experimental Study of Brillouin Frequency Shift on Classical and Modern BOTDA, BOTDR Setups''** completed by **Abdullah Erkam Gündüz** under supervision of **Prof. Dr. Halim Haldun Göktaş** and we certify that in our opinion it is fully adequate, in scope and in quality, as a thesis for the degree of Master of Science.

Prof. Dr. Halim Haldun GÖKTAŞ

(Supervisor)

Prof. Dr. Fatih Vehbi ÇELEBİ

(Jury Member)

Assoc. Prof. Dr. Murat YÜCEL

(Jury Member)

Prof. Dr. Fatih V. ÇELEBİ

(Director)

Graduate School of Natural and Applied Sciences

ETHICAL DECLERATION

I have prepared this thesis in accordance with the Rules of Writing Thesis published by The Graduate School of Natural and Applied Science of Ankara Yıldırım Beyazıt University;

- Data I have presented in the thesis, information and documents are obtained in the framework of academic and ethical rules,
- All information, documentation, assessment and results are in accordance with scientific ethics and morals,
- I have given the references for all the works that I used for in this thesis,
- I used the data obtained from the experiments without any change and modification,
- I declare that the work presented in this thesis is original,

I understand that all the rights and privileges earned through this thesis can be taken back in the event that any parts of the above declerations are found to be untrue.

EXPERIMENTAL STUDY OF BRILLOUIN FREQUENCY SHIFT ON CLASSICAL AND MODERN BOTDA, BOTDR SETUPS

ABSTRACT

Brillouin scattering has many applications in optics. This thesis study is observing the effects of various optical elements and environmental factors Brillouin gain spectrum and frequency shift on different optical configurations. Methods to improve Brillouin readings in classical and modern BOTDA/BOTDR configurations are proposed. Effects of EDFA power on Brillouin gain spectrum are observed on a BOTDA setup with single mode fiber as FUT. Comparisons with respect to optical Rayleigh power are done. EDFA power interval for sufficient Brillouin gain is obtained. Then, effects of step increments of ambient temperature on Brillouin frequency shift are observed on a BOTDR setup with single mode fiber as FUT. The relation between temperature and Brillouin frequency shift is obtained. In addition, effects of test fiber length on Brillouin gain spectrum are observed on the BOTDR setup. The direct relation in between Brillouin power and fiber length is observed. Furthermore, different length and brand fiber cables are connected back to back and their Brillouin frequency shifts are observed. Brillouin gain spectrum for fiber very short fibers (40m) is obtained.

Keywords: Brillouin Scattering, BOTDA, BOTDR, Rayleigh Scattering

BRİLLOUİN FREKANS KAYMASININ DEĞİŞİK KLASİK VE YENİ BOTDA VE BOTDR DÜZENEKLERİNDE İNCELENMESİ

ÖZET

Brillouin saçılması optik düzeneklerde pek çok uygulama alanına sahiptir. Bu çalışmada, çeşitli optik devre elemanlarının ve çevresel unsurların, Brillouin şaçılması güç değerleri ve frekans kayması üzerindeki etkileri farklı optik düzeneklerde incelenmiştir. Brillouin değerlerinin klasik ve yeni BOTDA/BOTDR düzeneklerinde daha etkili şekilde elde edilebilmesi için öneriler sunulmuştur. İlk olarak tek modlu test fiberi olan BOTDA düzeneğinde EDFA güç düzeyinin Brillouin gücü üzerindeki etkisi incelenmiştir. Elde edilen Brillouin gücü, farklı EDFA güç düzeylerinde optik Rayleigh gücü ile kıyaslanmıştır. Yeterli derecede Brillouin gücü sağlayan EDFA güç aralığı elde edilmiştir. Sonra, tek modlu test fiberi olan BOTDR düzeneğinde basamak basamak artırılan çevre sıcaklığının Brillouin frekans kayması üzerindeki etkisi incelenmiştir. Sıcaklık ve Brillouin frekans kayması arasındaki ilişki elde edilmiştir. Bununla birlikte, aynı düzenekte test fiber boyunun Brillouin gücü üzerindeki etkisi incelenmiştir. Fiber boyu ve Brillouin gücü arasındaki ilişki elde edilmiştir. Ayrıca farklı uzunluktaki farklı tekmodlu fiber kablolar uçuca eklenerek oluşturulan test fiberinde Brillouin frekans kayması incelenmiştir. Çok kısa fiber boyları (40m) için Brillouin güç spektrumu elde edilmiştir.

Anahtar Kelimeler: Brillouin Saçılması, BOTDA, BOTDR, Rayleigh Saçılması

ACKNOWLEDGEMENTS

I would like to express my sincere thanks and appreciation to my supervisor Prof. Dr. Halim Göktaş who offered this topic to me, taught, and guided me at each step throughout my study. I also thank to Prof. Dr. Fatih Çelebi and Assoc. Prof. Dr. Murat Yücel for their suggestions and helpful criticism. Finally, my thanks go to my family and my friends for their continuous supports.

2016, 10 November **Abdullah Erkam GÜNDÜZ**

CONTENTS

ABBREVIATIONS

APC	Angled Physical Contact
BOTDA	Brillouin Optical Time Domain Analysis
BOTDR	Brillouin Optical Time Domain Reflectometer
DFB	Distributed Feedback Laser
EDFA	Erbium Doped Fiber Amplifier
FC	Ferrule Connector
FUT	Fiber Under Test
TLS	Terrestrial Laser Scanning
SMF	Single Mode Fiber

LIST OF TABLES

LIST OF FIGURES

CHAPTER 1

INTRODUCTION

Fiber optic sensor is a rapidly developing research area. There are numerous studies, research and commercial applications abroad; however, this technology is new in Turkey. The loss factors that adversely affect optical data transfer actually provide sensory applications.

D. Hazarika and D. S. Pegue's work suggests using a microcontroller to monitor the air pressure with fiber optic sensors. A laser source is introduced to the system to improve the macro bending. A beam splitter, multi-mode fiber optic cable and light-dependent resistors (LDR) comprises AT89S8252 microcontroller circuit. One of the fibers is chosen as reference point to eliminate the environmental impact during the measurement of air pressure [1].

P. B. Buchade's study suggests a mobile platform can be designed and tested with an optical fiber sensor. IC 89C51RD2 microcontroller is used. The microcontroller on the platform, is designed with two motorized wheels behind and in front of a free turning wheel. Platform is equipped with weight sensors and plastic fiber touch sensor. The load cell sensors detect the current positions of the sensor (i.e. target), the proximity sensor and the weights. The route to reach the target position is deduced without any software on the platform [2].

In Alberto J. Palma and his colleagues' work, an optical sensor with portable optic-chemical electronic device for the detection of atmospheric oxygen is presented. Optical sensors based on luminescence quenching are designed. The sensor designs provide a single-channel optical sensor, an optical filter, a digital signal processing capacity, re-programming ability, data saving, low power consumption and high signal data processing rate. Digital output of the photodetector provides fewer harmonic terms and better noise reduction. Typical measurement range is from 0 to 30% oxygen, and the response time is under 30 seconds for the full range. It provides temperature correction and oxygen concentration accuracy of 0.5% [3].

In Mahfooz Rehman's study, the development of a low-cost intelligent fiber optic based liquid flow measurement system is discussed. A turbine is used as the flowmeter. Turbine blades are used to receive incident light onto the module. The frequency of the pulses produced depends on the number of blades. With the right calibration, the flow rate is almost linear and accuracy is 4% [4].

In Omar A. F. and M. Z. Matjafr's study, fiber optic spectroscopy method is used for detecting water quality. The system can detect the interaction between the scattered light and the suspended solids in water. The analysis (mg/L) is performed by measuring the density of suspended clay in the water. System is sensitive to blue (470nm) and red (635nm) monochromatic light. Two separate light detector circuits, TSLB257 and TSLR257 at the center of the sensor system have 470 nm and 635 nm peak responses respectively. The detection results are sent to the Basic Stamp 2 microcontroller for processing and analysis. The turbidity level is calculated by the microcontroller and displayed [5].

In Ryder's study, a stable, low-voltage detector, silicon photo mixer for measuring low light levels is discussed. These are designed for detecting high-altitude cosmic rays. In laboratory tests, embedded wavelength shifting fibers are used as cosmic ray detector. ARM Cortex-M3 detector that has been developed using a microprocessor-based data collection system [6].

In Qiuhong Zhang Qian's study, a computer system providing an information service and management system to improve the high-tech living stantdards of intelligent home control systems is discussed. Optical scattering based fiber sensor sensitive to temperature and stress changes is proposed. The microcontroller centered smart home control system with GSM and fiber optic sensor is explained. The study was conducted using the GSM wireless data transmission network for wireless communication [7].

In Zhang and Jiahong's study, a new method to control intensive electric-field measurement using asymmetric Mach-Zehnder interferometer-based LiNbO3 photonic sensor is proposed. With a microcontroller, an adjustable laser wavelength is obtained. The electrical field measurement is done with the linear operating point

of the sensor. This method performs successfully without disturbing the optical output wavelength of LiNbO3 photonic sensors. With the proposed control system linear characteristic of this detection system can vary from 840 and 160 kV / m to obtain a correlation coefficient of 0.999. This wavelength calibration technique is used to accurately identify and extract the electric field [8].

In Oleg Uzenkov's study, an FPGA based, fiber Bragg grating sensor system is proposed to measure the tension output. The system can track up to 10 simultaneous light source outputs generated by the fiber Bragg grating sensor with monochromatically tunable miniature. A 2048 pixel linear CCD array is controlled by the FPGA with 2 MHz scan frequency linear sequence and the first sub-pixel resolution is achieved. Control circuit to observe micro tensile equal to the resolution is performed by a XCS40, with 58% less logic resources [9].

In Graham Wild's study, a general purpose, smart transducer interface module for distributed optical fiber intelligent sensors (STIM) is designed to be used with intensio-metric fiber optic sensors. The system consists of two optical fiber interfaces, PIN receivers, a differential amplifier and a digital signal processor. Both of the received signals are strengthened to improve the signal-to-noise ratio and the differential sensitivity. DSP card has the ADC. This system has been successfully used in embedded systems as well as temperature and strain measurements. It can monitor and alert when a predetermined threshold is exceeded. Detection system used for dynamic strain signals also performs successfully without the DSP [10].

In Altuğ's thesis work, a fiber brag grating-based sensor system to measure the ECG signal of a patient is proposed. The signal is transferred via fiber optic media to the central control unit (i.e. computer). The control unit converts optical signal into electrical signal with a demodulator and a capture card data (Data Acquisition Card). The ECG signals are sampled rapidly and a database with this information is created. The control unit is also simulated with MATLAB. These projects can be created with the help of ECG follow-up networks. Synchronization with new technology can be provided if necessary. In addition, a human's heart health status throughout his/her life can be traced and monitored with a central database [11].

In Qin’s dissertation, a distributed optical fiber vibration sensor has been developed based on the Rayleigh scattering. The maximum distance between the vibration source and the detection point was measured to be 18 cm with a spatial resolution of 1 m. Distributed vibration measurements up to 500 Hz and 1 kHz were performed over a 20 cm length of single mode fiber [12].

In Karaman and Ünverdi’s study, different types of fiber Bragg grating-based optical fiber sensors are analyzed. The characteristics that make up the grid, reflection and transmission spectrum bandwidth were investigated. The reflected and transmitted power amount of the grid changes depending on the grid length and refractive index value, the temperature and stress. The amount of change occurring in the reflected wavelength is determined [13].

In Bao and Chen's study, the recent developments in scattering based fiber sensors are examined. The interaction of photons in the fiber with respect to temperature and stress is examined and corresponding Rayleigh, Brillouin and Raman scattering intensities are observed. These local temperature and stress variations cause interactions resulting with acoustic/mechanical waves with a dynamic viscosity diversity. The phase, frequency and amplitude changes of the scattered back light on hundreds of meters of the fiber can be analysed to find the vibration measurement [14].

In Soto’s study, Brillouin optical time domain analysis (BOTDA) with optical pulse coding techniques for long-haul distributed sensors are examined. Compared with conventional BOTD sensors, optical coding offers a better detection range and 1 m margin of error over 50 km of single-mode fiber. It also offers better temperature and stress measurements [15].

In Hao’s study, return to zero/not return to zero (RZ / NRZ) formats are used for long-distance optical probe pulses with low margin of error measurements. The detection ranges increase with the use of zero-return format. 512-bit coded pulses are sent to 50 km fiber and the voltage measurements are performed with 0.5 με accuracy [16].

In the study of Barrios, Brillouin sensors are discussed to offer innovative solutions for temperature and strain measurements on large structures. Typically, Brillouin optical time domain analysis has effective measurement range of 20-30 km interval. BOTDR approach is tried for the sensor. The measurement quality can be increased as well as the measurement range [17].

In the study of Soto, using long-distance and Raman amplifier to achieve high-resolution measurements with Brillouin the time domain analysis (BOTD) is examined. 120 km long single mode fiber with a Raman amplifier reinforcement is used. The error margin was low with 45με and 2m/2.1°C accuracy of stress/temperature measurements [18].

In Jia' study, Brillouin optical time domain analysis (BOTDA) with Raman amplifier approach is used for achieving high performance, high accuracy temperature measurements. The experimental results confrimed theoretical assumptions. Raman amplified temperature measurements are conducted with 0.6 ° C error margin along the 75 km fiber. The broad Raman power and Brillouin pump power help to improve the signal to noise ratio. Raman amplification makes it possible for BOTDA to be used in long distances and as potential fire alarm sensors [19].

In Zornov's study, for hybrid and combined Brillouin distributed sensors, a new Raman amplified consept is proposed that has long range sensing with low cost. On a 46 km network, point vibration sensors and temperature sensors are distributed over fiber brag gratings. In order to tolerate for 13 m spatial resolution and 0.7 °C temperature measurements, Raman amplifier is used. Density sensor are also able to measure vibrations in the frequency range of 0.1 Hz to 50 Hz [20].

In Sperber's study, a new BOTDA technique that is capable of taking measurements in the spatial resolution range of few centimetres is developed. This technique requires only a single long pump pulse for the acoustic wave and is based on a simple modulation scheme. Brillouin frequency changes are experimentally detected with 2cm spatial resolution [21].

In Chen's study, a new distributed sensor structure that is dependant on the relationship of Brillouin gain and loss is discussed. Using 20/15 ns Stokes and anti-Stokes pulses on a 15 m polarization protected fiber, a spatial resolution of 0.5 m and 6 με stress is obtained experimentally [22].

In Mafang's thesis, a new technique called Brillouin scattered resonant detection (BEDS- Echoes Distributed Brillouin sensing) is discussed. First, the classic Brillouin sensor configuration is updated. Then constraints encountered in conventional Brillouin sensors at long distances are examined. Secondly, BEDS approach to identify the spatial resolution in Brillouin scattered measurements are presented. It was possible to achieve greater accuracy with lower error rate in laboratory testings using BEDS technology. In addition, using BEDS fluctuations along the photonic crystal fiber, its geometry is modeled [23]

In Foaleng's study, high spatial and spectral resolution in detecting Brillouin, optical phase control and activation by using acoustic wave are discussed and signal to noise ratio is examined. Acoustic wave activation maintains its natural Brillouin wavelength, whereas it uses different gain techniques. 3 MHz resolution over 5 km of fiber, 500 psi (5 cm) is measured using the phase shift of the Brillouin shift frequency coupling is carried out experimentally [24].

In Andrew's study, nonlinear change in stimulated Brillouin scattering in a single-mode fiber is observed experimentally. At high laser excitation, equal to half of Stoke impact on the earnings outlook of traditional fiber Brillouin frequency was investigated [25].

In Alahbabi's study, to improve the performance of distributed temperature and voltage sensors based on Brillouin scattering, random compatible detection studies are conducted. To increase the detection range and the performance of the sensors, Raman amplifier with different Raman pump configurations are examined. Using only Raman diffusion pump, the frequency measurements are performed with a 150-km fiber at 50 m spatial resolution and temperature measurements with a resolution of 5 °C. Spread along 100 km of fiber in the Raman pump with 20 m resolution and 1.7 °C resolution temperature offspring are achieved. Together with the use of power

and frequency of the Brillouin signal, 50 km fiber for 3.5 °C temperature resolution and 85με voltage error of 5 m is identified [26].

In his thesis, Günday discussed, in order to reach the temperature data along the cable, temperature measurement method based on Raman scattering is used. Brillouin frequency shift is utilized to obtain data for the fiber's temperature and stress. Experimental temperature and strain measurement data for 380 kV power cables are obtained using 5 km long single-mode fiber at 1550 nm wavelength [27].

In Günday's study, the temperature and strain detection simulations along 380 kV high voltage cable at 1550 nm single-mode optical fiber are performed. To reach the temperature data along the cable, distributed temperature sensing based on the Raman scattering method is used. In order to obtain strain data over cable, i Brillouin frequency shift of the backscattered signal is used. For cable joints, intersections and other passage of pipes under, a 5 km long fiber is used. The simulation results are 1.5 m spatial resolution 1.25 °C temperature resolution and 50με strain resolution. In addition, utilizing the Brillouin frequency shift and Brillouin gain spectrum change profile along the cable, the effective value of the frequency shift noise 1:20 MHz and power exchange RMS noise on cable is calculated as 0.45% to [28].

In Frazao's study, Raman fiber bragg grating stress sensor for temperature measurement are presented. Using a 35nm pump Raman laser, bragg grating sensor is achieved. Bragg gratings determined by a 10 km radius from the detection system is run [29].

In Martins' study, along with Rayleigh scattering, a fiber bragg grating Raman laser FWM (Four-Wave Mixing) is proposed to obtain a voltage-based temperature sensor. To strengthen their Raman and Rayleigh scattering along two linear fiber bragg grating laser sensor is used to format the space. Because of the low fiber dispersion coefficient, it was possible to use two lasers using FWM. In this configuration, only one of the two sensors are sensitive to voltage. The difference in the converted signal by the wavelength of the signal sensor 2 pm / με offers a stress factor in sensitivity [30].

In Koyamada's study, the OTDR is used for distributed strain and temperature measurements. Using this technique, 8 km length of 0.01 °C precision temperature measurements were made in a fiber [31].

In Alahbabi's study, Raman amplified Brillouin scattering based distributed temperature sensor with extended frequency offset detection is studied. With 100 km, Raman pump, 0.8 °C temperature sensing accuracy is achieved. With 150 km emission-free Raman pump, 5.2 °C temperature sensing accuracy is achieved and the location of the change is detected with 50 m accuracy [32].

In Li Yuelu's study, using a optical time domain reflectometer (OTDR) a phase diffuse vibration sensor is developed. Broadband acoustic frequency vibration components are generated by breaking the pen. These vibration sensors measured the scattering. The fracture is a standard technique for pre-defined acoustic analogy for pen breaking measurement of steel or concrete bridges. 1 kHz frequency response with 5 m highest point accuracy is obtained [33].

In Gifford's study, a fiber optic temperature sensor based on Rayleigh scattering's temperature and spectral shift is developed. Wavelength scanning interferometer is used to measure the Rayleigh scattering [34].

In Posey's study, a fiber optic strain sensors based on optical pulse using the time division multiplexing Rayleigh scattering is developed. This sensor in a small adjustment range of 2 kHz and has a small stress sensitivity of 0.5 m [35].

In Signorini's study, gradient index multimode fiber and high performance based on standard single-mode fiber distributed temperature sensing system developed for Raman techniques are presented. The code generated by this technique offers opportunities for a very long measurement capability for spatial resolution [36].

Long-distance fiber-optic Raman sensors work by Farahani and Gogolla is used for distributed temperature measurement. For this purpose, the optical fiber frequency domain reflectometry is applied. Theoretical Raman intensity of single-mode and multi-mode fibers are formed. Thus, wavelength for a suitable sensor for optical fiber

Raman sensing element is determined. In addition, errors in temperature sensor for long fibers are analyzed theoretically [37].

In the study conducted by Bello and Vo-Dinh, stimulating and supported collector surface Raman scattering (SERS) in a fiber-optic system has been developed for the signal. Fiber type to be fulfilled in optimum conditions SERS fiber-optic devices, fiber substrate geometry and other experimental parameters are investigated. In addition to measuring the performance of the SERS fiber-optic sensors, linear dynamic range, reproducibility, various parameters such as detection limit are examined [38].

In Hartog's study, the design of a fiber-optic distributed temperature sensors, operating principles and performance was examined. The backscattered power to detect temperature changes in more than one point on the fiber optic time domain reflectometer (OTDR) is used. In a study conducted over a fiber length of 100 m and 1 m spatial resolution of 1 ° C measurement accuracy of the temperature detection are performed [39].

In Al-Tahir's study, Rayleigh scattering from a 22 km long fiber and multipoint fiber brag grating (FBG) with a Raman fiber laser reflector is observed. 100 GHz spaced 22 laser line has been established. Established circuit has shown that it is possible to create Raman gain width of about 100 nm [40].

In Bologna's study, coded behavior of distributed temperature sensor based OTDR has been studied theoretically and experimentally. In particular, high performance, using the appropriate amplitude modulation to simplex coding design has been applied. Partly Raman amplification and detection range is expanded by using a direct detection. 17m spatial resolution of 30 km and with 5 K temperature resolution scattering shifted along the fiber, efficient and proven economic theory and a distributed temperature sensor has been achieved experimentally [41].

In Stokes and Vo-Dinh's work, surface dependant Raman scattering based (SERS-Surface Enhanced Raman Scattering) fiber sensor for remote measurements is developed. The heart of the sensor is designed with a special single-mode optical

fiber. Based on a single fiber offers practicality specially designed for measuring displacement in the microenvironment, remote type sensor for SERS signal is carried along the laser excitation and radiation parameters in a single fiber is simpler and more stable [42].

Palmieril and Schenato's study features scattered fiber sensors based on Rayleigh scattering. This scattered optical sensors are based on the interaction between light from scattering processes occur and objects. This work may occur in fiber Rayleigh, Brillouin and Raman scattering from Rayleigh scattering sensors based on optical fibers are examined. For a given optical frequency, intensity Rayleigh based sensors with three fundamental characteristics of light, it uses the phase and polarization. All these detection mechanisms in this study basic principles, the basic flow is analyzed in terms of techniques and applications [43].

In Froggat's study, a Rayleigh scattering-based distributed measurement technique has been developed. Using standard fiber polarization voltage and the detection of temperature change was investigated. Scattering of the desert in high-precision optical frequency domain reflectometry that is used [44].

In Newson' study, Rayleigh and Brillouin scattering's intensity dependence on the temperature is observed experimentally. These results will allow the random result of temperature and strain the construction of Brillouin scattering distributed fiber sensor that measures the temperature and stress when they occur combined with the frequency dependence of the Brillouin scattering known [45].

In Ji Han Lee's study, Raman amplification based on random temperature and voltage measurements are analyzed. For this erbium doped fiber (EDF) and a detection probe consisting of the combination of fiber brag grating it is used. These measurements are used for fiber 50 km long, 11 dB signal to noise ratio (SNR), high-quality signal could be detected [46].

In Kazuo Hotate's study, Brillouin dynamic grid (BDG) and using the Brillouin scattering together, distinctive and heat stress with techniques BOC held its messy 10 mm resolution measurements [47].

In Wosniok's study, stretching a single mode along the fiber is developed. Distributed fiber optic monitoring system for determining the temperature is based on the BOFD technical and no frequency interference effects using sideband technique is being used. By a single DFB laser to cut costs been and is not necessary to set the laser source [48].

In Hyungwoo Kwon' study, 36 km length of coherent along the fiber line (one-stage) using a detection system of long-distance dispersed measuring system have been developed. Using the optical modulator (AOM) the damping ratio in optical pulse is developed. The result, which applied to optical fiber temperature and strain, calculated using the Lorentzian algorithm, the Brillouin frequency shift has also been successfully measured [49].

In AH. Resham's study, optical fiber in Brillouin and Rayleigh scattering behavior are examined. Simulating dominant noise source of coherent Rayleigh noise (CRN) calculating is done. Analyzing temperature and stress result thanks to algorithm characteristics are examined. Thanks to a new algorithm, the position of the Brillouin backscattering can be effectively found for a pump power known [50].

In Yosuke Mizuno's study, to diffuse tension measurement BOCD technique as high Brillouin gain a tellurite glass fiber is used. First, BOCDR by use of the gain fiber is evaluated. High Brillouin spatial resolution using tellurite fiber has clearly the spatial resolution Rayleigh scattering - using fiber is restricted. By inducing noise, BOCD the Brillouin frequency shift with the technical 6 mm spatial resolution of 1 cm was measured at a tensile successfully applied field [51].

In Yunqi's study, BOTD detection system in spontaneous Brillouin scattering spectrum of the signal to noise ratio (SNR) examined the development impact of theoretically and experimentally the effects of changing the modulated pulse shape is given. Same pulse width or the same spatial resolution, SNR is greater than the impact triangular contraction and sensing distances of the spectral width. Meyd has nearly doubled the triangular instead of rectangular pulses using pulse [52].

Romeo Bernini and colleagues' work suggests temperature / stress measurements for the full frequency base of optical fiber Brillouin sensing techniques to experimental verification is shown. The signal to noise ratio is developing both long distance in the deal with the effects of non-regional occurring while measuring, sensing fiber Brillouin gain profile and along they offer an original formula in the form of base frequency related measurements [53].

In Y. D. Gong's work, optical stimulated in the fiber Brillouin upgrade impact based distributed temperature and place the analysis of the stress sensor is given. Our starting power, such as optimizing the design guide of the short and long-distance distributed temperature and strain sensors offers some new rules [54].

In V. Lecoeuch's study, 25 km from the sensors in the length of fiber in any of 2 m on the applied temperature or stress is perceived quickly enough some precision, a new study stimulated Brillouin scattering-based single-ended to a fiber sensor is shown. The study also phases modulation effect; the probe reveals the impact a major limiting factor for wave power [55].

In P.C. Waite's study, narrow bandwidth pulse advances in laser technology and low-loss fiber filters through Brillouin signal can be separated from the Rayleigh signal. Theoretical analysis, Brillouin scattering-based spontaneous temperature sensing Raman-based sensor indicates that provide longer detection of the system [56].

In Shekhar and P. K. Pradhan Sahu's study, BOTD based for optimization is shown. The receiver performance improvement of 150 km of scattered sensor system, phase modulation and a global transformational calculation based optimization technique (Differential conversion algorithm (DE)) a BOTD system formed by the combination. 150 kilometers detection compared with an amplitude modulated wave probes have provided 3.3 dBm for distance like a SNR improvement [57].

In Haroldo T. Hattori' work, smart materials and scattered detection for buildings Raman and Brillouin effects of that custom applications. In the types of sensors, fiber that acts like a messy sensor kilometers stretching across the length and temperature

can be detected at the same time to process this information, the data also show that fiber can carry the Brillouin and Raman systems for the optimization is started, to cover long distances in a small area of effect. Hence special elliptical fiber sensor and is intended for use in low-power laser [58].

In Xue-Feng Zhao's study, asset-based thermometers scattered Brillouin optical sensor used in submarine pipeline monitoring system is discussed. The system shows direct heat exchange, heating and a parallel thermal cable to the pipeline provides the frequency shift of the optical sensor during cooling. Collapse scenarios and welded release stress is tested. Temporal stability of the different behavior of water in heat transfer, the three-feature temperature-time history including spatial continuity and size are obtained. The experimental tests have proven the system can run over a monitoring system [59].

In Lijuan Zhao's study, 110 kV fiber composite submarine cable with 1 m spatial resolution with BOTD established system is observed. The system in China now also offered. Spring monitoring system provides an appropriate plan to ensure the safe operation of the submarine cable [60].

In V. Lecoeuch's study, high-grade Stokes and the suppression of anti-Stokes components and very high conversion a Brillouin fiber used grid Bragg for efficiency laser configuration is presented. Theoretically presented a study and experimental feasibility proven its operating system to reduce the laser bandwidth and it provides a technical solution in reducing noise [61].

In A. Perez-Herrera and M. Lopez-Amour's study, including networks using optical amplification and lasing multiplexing systems, which define the different types of multiplexing networks used in fiber optic sensors and compared. Especially healthy and should focus away from the multiplex network and dispersed scattered Brillouin sensor networks has been shown [62].

In Bum Kwon's study, dozens of kilometers an overall laser diode. To construct a compact BOTD detection system intrusion along the line detection and is capable of showing the location and two electro-optic modulators are used. Affect of an attack

simulation, stress that a device to obtain 4.81 kilometers in length edilmiştir.1.5 secs is provided with a resolution of 3 m optical fiber [63].

In Shiqing's study, an iron mine located in my southern part of the city as a physical and mechanical testing model to investigate the collapse of a portion of the earth's surface to monitor. Modelling the stress distribution according to BOTD technique is used. Test result BOTD based scattered detection high sensitivity of the method, easy handling, good tensile testing techniques because of their advantages such as immunity to interference are that it [64].

In Zhou's study, to monitor the characteristics and state of stress damage to the ice structure as shown. As an early warning system, a block of ice and ice rafter's load under axial and bending to understand the behavior of the fiber Bragg grating and BOTDA/R sensors are placed. Second, damage to the ice structure under test conditions and the accuracy of the claims process as early warning damping systems edilmiştir.so obtained analytically and ice structure of the behaviors were monitored continuously for 34 hours. Ultimately, optical sensor long-term structure of the ice early warning system has been shown to be effective in monitoring [65].

In Femi Tanimol and David Hill's study, formerly Fixture has LNG and from giving examples leak detection systems used in LPG pipelines fiber optic distributed temperature sensing (DTS) leak made using identified and explained third parties' burglary detection system principles. As a result, fiber optic acoustic sensing scattered next to pipelines that provide the environmental protection, efficiency and integrity (DAS) burglar monitoring system has been examined [66].

In Si Zhu Yan and Lee Sheng's study, stimulated Brillouin scattering (SBS) threshold, sensing distance, the signal is noise ratio and the critical parameters in the pipeline for the performance of BOTD system of the concept of spatial resolution that is used. According the study, the optical fiber nonlinearity, statistical approach stimulated by the Brillouin results of simulations until the theoretical approaches along with concepts such as scattering is used. The result, SBS to print up to 11 dB maximum sensing distance of the next 110 km/s far are shown. 3-bit simplex coding working laser pulses to improve the SNR at the receiving end according to the results

are used. Simulating 1:38 SNR gain and higher SBS threshold has been observed [67].

In Yingchun Ding's study, scattering Brillouin stimulated in different frequency optical fiber (SBS) two continuous waves generated by (CV) waveform are shown. signal pulse shape control of the pulse signal by using experimentally depending on total input power "fully optical" way module methods have provided a novel method not only for light nanosecond pulse width for control of the light is available [68].

In Yucel's study, the temperature effects on fiber's Brillouin gain spectrum and frequency shift are observed. A BOTDR setup is used. 40m length fiber under test is exposed to temperatures 22ºC and 95ºC. Then, using an RF analyzer the Brillouin gain spectrum is observed. A 1°C/0,921 MHz temperature change is observed [69].

In Öztürk's study, a Fiber Bragg Grating (FBG) based temperature sensor is analyzed and simulated. FBG is gradually exposed to temperatures from 0ºC to 60ºC in 10ºC steps and the frequency shifts in both RF and optical spectrum are observed. A 10 ºC/0.1 nm wavelength change is obtained [70].

Since Brillouin scattering holds an important place in fiber sensor applications, it is important to analyse Brillouin gain spectrum and frequency shift very accurately. In this study, various factors that may affect the Brillouin gain spectrum and frequency shift such as, EDFA power, fiber length and ambient temperature are observed.

CHAPTER 2

THEORY

2.1 Optical Scattering

2.1.1 Linear Scattering

2.1.1.1 Rayleigh Scattering:

The inhomogeneous molecular structure of the silica glass causes random refractive index fluctuations. The resulting scattering field is proportional to ω^2 hence the scattered wave is proportional to ω^4. This means that waves with lower wavelengths are scattered much more [71].

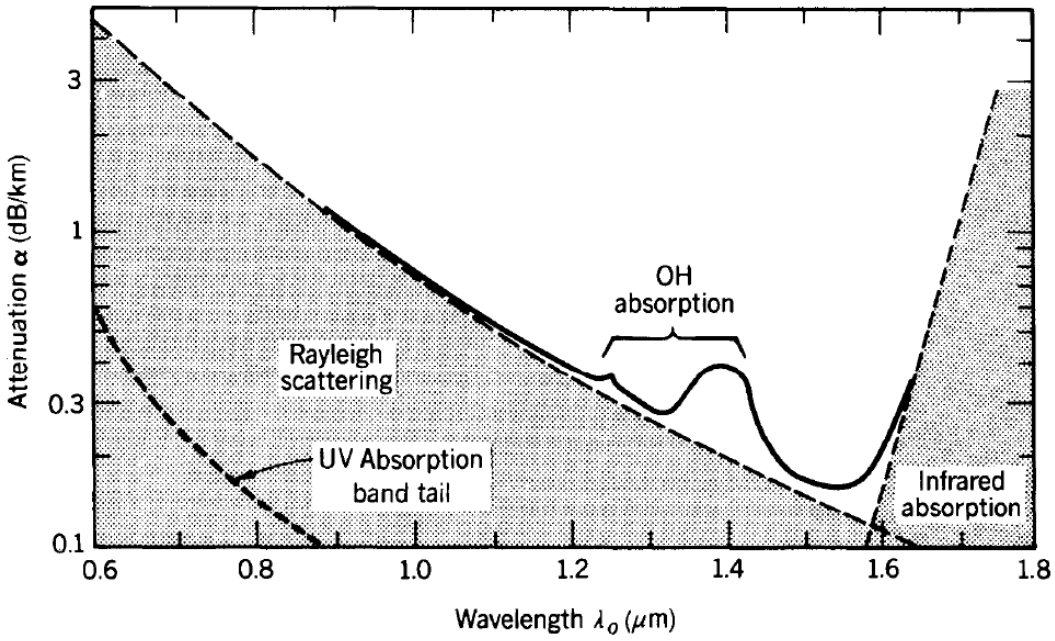

Figure2.1 Rayleigh scattering vs. wavelength [71]

The electric displacement field vector for fiber can be written as:

$$\mathbf{D} = \epsilon_0 (1 + \chi) \mathbf{E} = (\varepsilon + \Delta\epsilon) \mathbf{E} \qquad \textbf{(2.1)}$$

The $\Delta\epsilon$ represents the molecular discrepancies. With the Maxwell equation for the electric field:

$$\mu_0 \varepsilon \frac{\partial^2 \boldsymbol{E}}{\partial t^2} - \nabla^2 \boldsymbol{E} - \boldsymbol{\nabla}[\, \boldsymbol{E} \cdot \boldsymbol{\nabla} \ln(\varepsilon + \Delta\epsilon)] + \mu_0 \frac{\partial^2 (\Delta\epsilon \boldsymbol{E})}{\partial t^2} = 0 \quad \textbf{(2.2)}$$

The Δϵ terms in above equation represent the scatterings that are both spatial and time dependent. Assuming only Rayleigh scattering, i.e. only considering time dependence, the equation can be simplified to:

$$\nabla^2 \boldsymbol{E} + \boldsymbol{\nabla}[\, \boldsymbol{E} \cdot \boldsymbol{\nabla} \ln(\varepsilon + \Delta\epsilon)] + \mu_0 \varepsilon \omega^2 (1 + \frac{\Delta\epsilon}{\varepsilon}) \boldsymbol{E} = 0 \quad \textbf{(2.3)}$$

The wave medium fiber means we need only to take z axis in consideration, the equation becomes:

$$\frac{\partial^2 \boldsymbol{E}}{\partial z^2} + \mu_0 \varepsilon \omega^2 \left(1 + \frac{\Delta\epsilon(z)}{\varepsilon}\right) \boldsymbol{E} = 0$$

$$\frac{\partial^2 \boldsymbol{E}}{\partial z^2} + \beta^2 \left(1 + \frac{\Delta\epsilon(z)}{\varepsilon}\right) \boldsymbol{E} = 0 \quad \textbf{(2.4)}$$

2.1.1.2 Mie Scattering:

Mie scattering, just like Rayleigh scattering, is the scattering that is caused by the inhomogeneities of molecules and particles in the fiber. Molecules and particles that are larger than the wavelength of the incident wave cause the Mie scattering. The forward Mie scattering is heavier for larger particles [72].

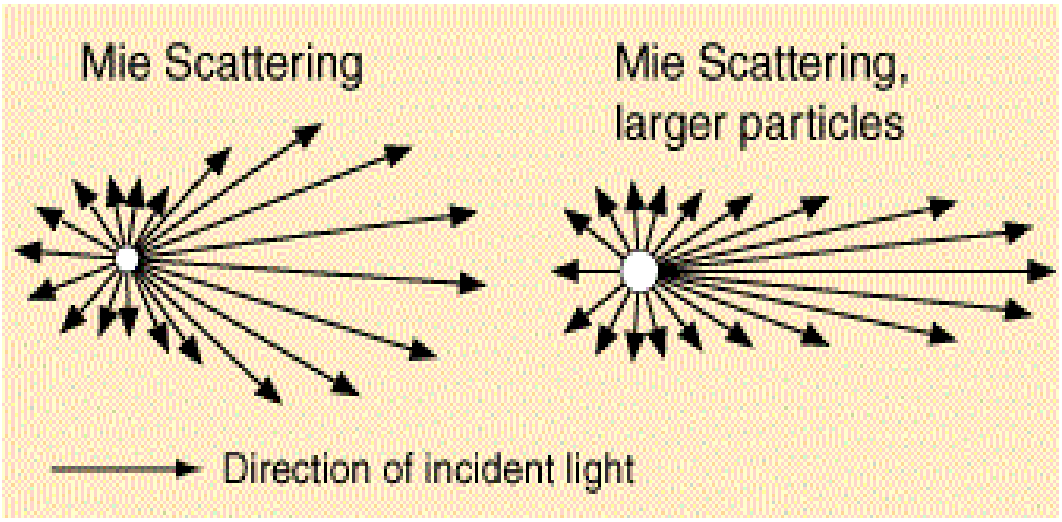

Figure2.2 Mie scattering in a silica fiber [73]

2.1.2 Nonlinear Scattering

2.1.2.1 Raman Scattering:

The incident light travelling through silica fiber excites molecules to higher energy states, where vibrations occur. These states have comparatively small energy levels such that the excitation must happen with the help of an additional photon transitioning to Raman. The first photon has frequency ω_p and the additional one has ω_s. If the vibrational state has energy ħ(Ω) at frequency Ω, the resulting scattering converting ω_p to ω_p - Ω (i.e., ω_s) is an inelastic process called Stokes. The transition from ω_p to ω_p + Ω on the other hand is called Anti-Stokes [74].

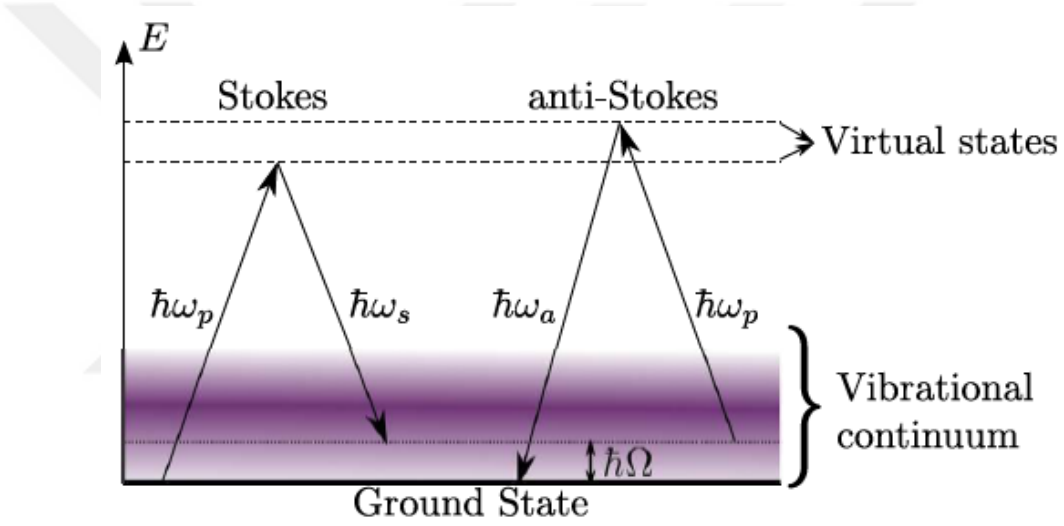

Figure2.3 Stokes and Anti-Stokes in a silica fiber [74]

The resulting vibrations can actually be treated as a third phonon with set frequency if you will. However, the set frequency does not obligatorily fall to ω_p- ω_s, hence the scattered light does not have a unique direction, rather random. The most of the energy however, is dealt among forward and backward scattering [74].

The Raman scattering can also convert the Stokes or Anti-Stokes scattered light back to original frequencies; ω_p or ω_s. This is called the reverse Stokes or Anti-stokes.

The pump light (ω_p) has the following power equation with the below thermal equilibrium (m_{th}) equation:

$$\frac{\mathrm{d}}{\mathrm{dz}} S(z,\omega) = \left[S(z,\omega) g\left(\omega_p, \Omega, \theta\right) + \frac{\hbar\omega}{2\pi}\left[m_{\mathrm{th}}(|\Omega|) + v(\Omega)\right] \left|g\left(\omega_p, \Omega, \theta\right)\right|\right] P_p(z) \quad \textbf{(2.5)}$$

$$m_{\mathrm{th}}(|\Omega|) = \left[\exp\left(\frac{\hbar|\Omega|}{k_B T}\right) - 1\right]^{-1} \quad \textbf{(2.6)}$$

$$g\left(\omega_p, \Omega, \theta\right) = g_{\parallel}\left(\omega_p, \Omega\right)\cos^2(\theta) + g_{\perp}\left(\omega_p, \Omega\right)\sin^2(\theta) \quad \textbf{(2.7)}$$

The g(ω_p, **Ω**, θ) provides the Raman gain which decides how strong a scattering happens. As mentioned above, the amount of gain is related to the polarization of light. Should the ω_p and ω_s happen to be linearly polarized, the Raman gain becomes maximum, while most of its energy is preserved in forward and backward scattering [74].

Stimulated Raman Scattering:

In addition to the pump (ω_p) beam, if there are any other linearly polarized beams, the resulting Raman scattering tends to be much stronger. This phenomenon is called the stimulated Raman scattering. The additional beam has the frequency ω_p - **Ω** or ω_p + **Ω**, hence, the scattered light will amplify this beam [75].

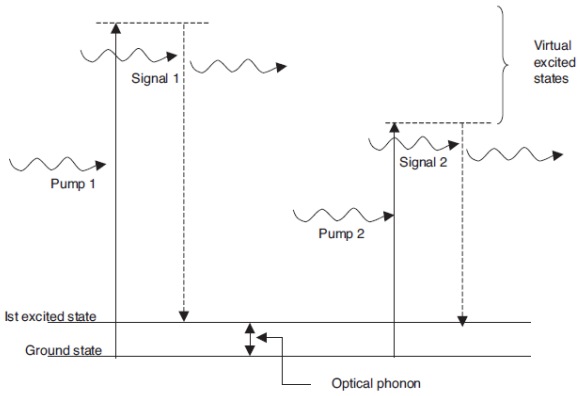

Figure2.4 Stimulated Raman scattering in a silica fiber [75]

Figure 2.3 shows a summary of the stimulated process. The inelastic polarization excites the molecules to the virtual state. With the additional light beam already on this excited state, it gets even stronger when scattered light is added. The amount of frequency shift (i.e. Raman ω_p - ω_s) highly depends on the material vibrational levels [75].

The resulting stimulated scatterings are temperature dependent and the strength of the scattering increases with higher temperatures. The Anti-Stokes scattering however, reaches 0 as the temperature gets lower, while stokes scattering saturates to a fixed level. Hence, the Stokes phenomenon would be quite useful in low temperature sensing applications [75].

2.1.2.2 Brillouin Scattering:

The Brillouin scattering has the same concept as the Raman scattering, except here the resulting vibrational state is sound waves not molecular vibrations. Brillouin scattering is polarization dependent and has much lower vibrational frequencies (~10GHz) compared to the Raman scattering [76].

The dispersion equation for acoustic wave in Brillouin scattering is:

$$|\Omega| = v_A |k_A| \quad \textbf{(2.8)}$$

v_A = 5.96 km/s is the velocity of acoustic wave and k_A is the wave vector.

The wave vector has to obey the conservation of momentum, therefore $k_A = k_p - k_s$, i.e. the difference between pump and Anti-Stokes waves. The magnitude of the wave vector can be found as:

$$|k_A|^2 = (k_p - k_s)^2 = |k_p|^2 + |k_s|^2 - 2k_p.k_s \quad \textbf{(2.9)}$$

The energy gap between pump and Anti-Stokes is miniscule, i.e. $k_p \approx k_s$, which means:

$$|k_A|^2 = |k_p|^2 + |k_s|^2 - 2k_p.k_s \approx |k_p|^2 + |k_p|^2 - 2k_p.k_p = 2|k_p|^2 - 2|k_p|^2\cos(\varphi)$$

$$= 2|k_p|^2 (1-\cos(\varphi)) \quad \textbf{(2.10)}$$

$$|k_A|^2 = 2|k_p|^2 (1-\cos(\varphi)) = 4|k_p|^2 (1/2-\cos(\varphi)/2) = 4|k_p|^2 \sin^2(\varphi/2) \quad \textbf{(2.11)}$$

Putting $|k_A| = 2|k_p|\sin(\varphi/2)$ into (2.8):

$$|\Omega| = 2v_A|k_p|\sin(\varphi/2) \quad \textbf{(2.12)}$$

where $|k_p| = 2\pi n/\lambda$, (n the refractive index and λ wavelength):

$$|\Omega| = 4\pi n \sin(\varphi/2)\, v_A/\lambda \text{ (Bragg condition)} \quad \textbf{(2.13)}$$

which has the maximum value when $\varphi = \pi$ (i.e. the pump and anti-stokes waves are at opposite directions); $|\Omega| = 4\pi n\, v_A/\lambda$ and minimum value for $\varphi = 0$, $|\Omega| = 0$ (no Brillouin scattering), meaning no frequency shift in forward direction.

The Brillouin frequency shift is $\omega_B = \Omega/2\pi = 2v_A|k_p|\sin(\varphi/2)/2\pi$. So at $\varphi = \pi$ we have the maximum frequency shift:

$$\omega_B = 2n\, v_A/\lambda \quad \textbf{(2.14)}$$

The Brillouin gain spectrum can be written as;

$$g_B(\omega) = \frac{g_B(\omega_B)}{1+(\omega-\omega_B)^2 T_B^2} \quad \textbf{(2.15)}$$

Which is a Lorentzian equation with maximum value at $\omega = \omega_B$, at backward direction. The T_B is the lifetime of acoustic phonons.

2.2 Brillouin Optical Time Domain Methods

2.2.1 Brillouin Optical Time Domain Reflectometry

Fiber sensor systems based on Brillouin scattering provide distributed sensing with the unique frequency shift of the backscattered light in the optical fiber. The reflected light has different frequency shifts with respect to the local fiber points. Applied strain and/or temperature to the optical fiber affects the Brillouin frequency shift. The relationships between BFS and temperature or strain can be described as;

$$v_B(T_r, \varepsilon) = C_S(\varepsilon - \varepsilon_r) + v_{Br}(T_r, \varepsilon_r) \quad \textbf{(2.16)}$$

$$v_B(T, \varepsilon_r) = C_T(T - T_r) + v_{Br}(T_r, \varepsilon_r) \quad \textbf{(2.17)}$$

where v_B is Brillouin frequency; C_S and C_T are strain and temperature coefficients, respectively; whereas T_r and ε_r are relative strain and temperature compared to a reference Brillouin frequency v_{Br} [76].

The BOTDR system acquires the Brillouin spectrum of the sampling points along the fiber path, and then the strain or temperature is determined using the relationship above. First, pulsed light is launched into one end of single-mode optical fiber while the other end of the fiber is left open. Then the Brillouin backscattered signal is obtained on the same end. The Brillouin backscattered light power $dP_B(z, v)$ that is produced in a small section, *dz*, of the fiber is:

$$dP_B(z,v) = g(v,v_B)\frac{c}{2n}p(z)dz \cdot \exp(-2\alpha_z z) \quad \textbf{(2.18)}$$

$$g(v,v_B) = \frac{h(w/2)^2}{(v-v_B)^2+(w/2)^2} \quad \textbf{(2.19)}$$

$$z = \frac{ct}{2n} \quad \textbf{(2.20)}$$

Where z is the distance along the fiber; *p(z)* is the launched signal power at z; c is the velocity of light in vacuum; n is the refractive index of the fiber; α_z is the attenuation coefficient of the fiber; t is time interval between the pulsed incident light and the backscattered light at the detector (i.e. doing so the location of the received backscattered light can be found) [76].

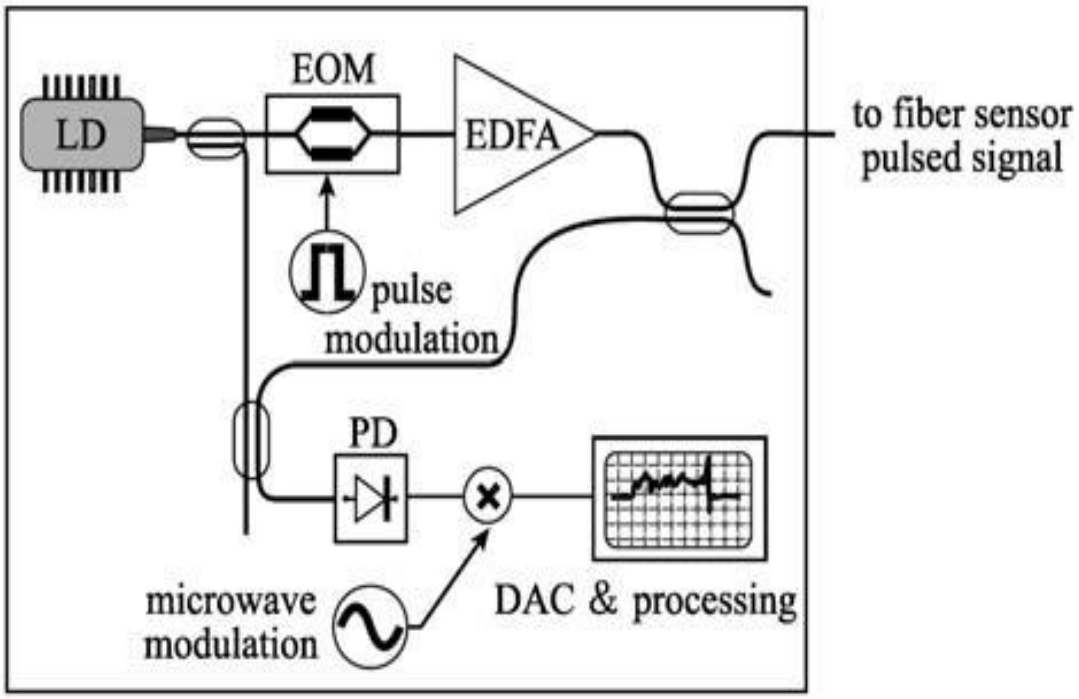

Figure2.5 BOTDR Setup [77]

2.2.2 Brillouin Optical Time Domain Analysis

Here, the stimulated version of Brillouin scattering is used and is based on a pump-probe technique. From one end of the fiber, an intense pump pulse is sent while; on the other end, a weak continuous probe wave is sent. The pump wave feeds the weak continuous wave and the gain experienced by the probe on each location can be deduced in the time domain. For each differential location, the frequency difference between pump and probe is scanned and a localized map for Brillouin gain is obtained.

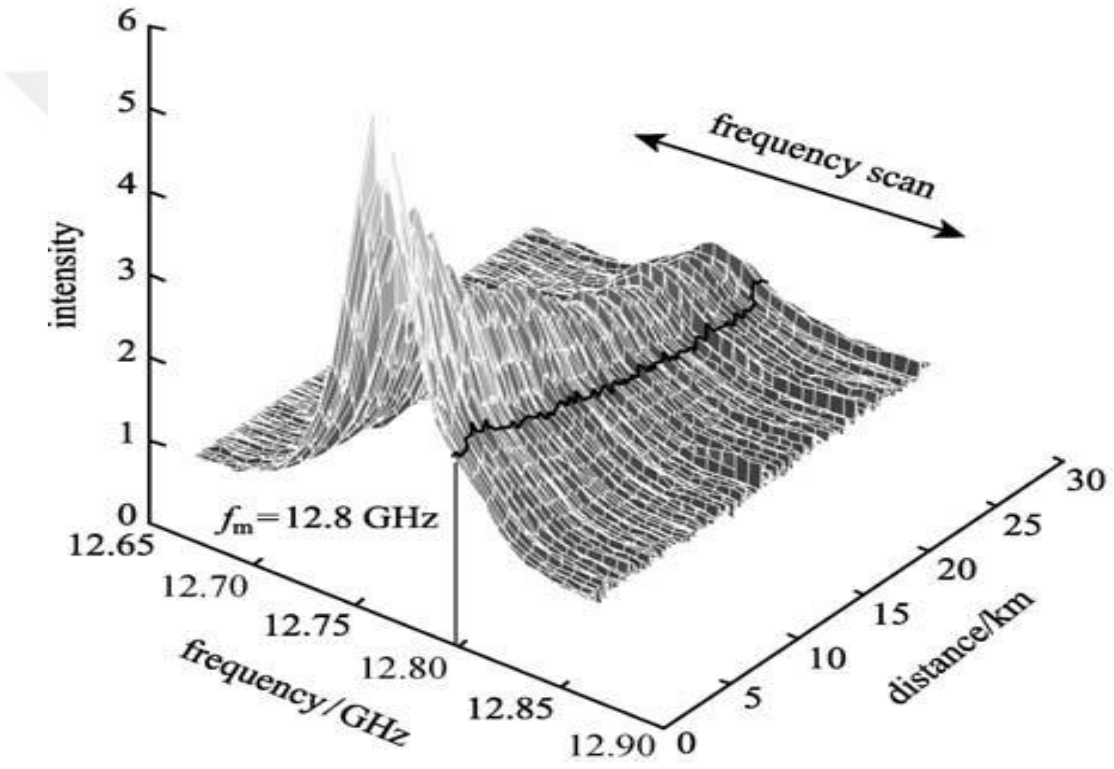

Figure2.6 localized Brillouin gain spectrum

The pump pulse and CW probe propagate in reverse direction to each other in the sensing fiber. In addition, the electrostriction that stimulates the acoustic wave is driven by the interference between pump and signal. Once their polarizations are aligned, maximum gain is obtained. Orthogonal polarizations, on the other hand, will result in a totally vanishing gain. In order to prevent zero gain, polarization scramblers may be needed. The polarization dependence may be useful in measuring local birefringence properties along the optical fiber.

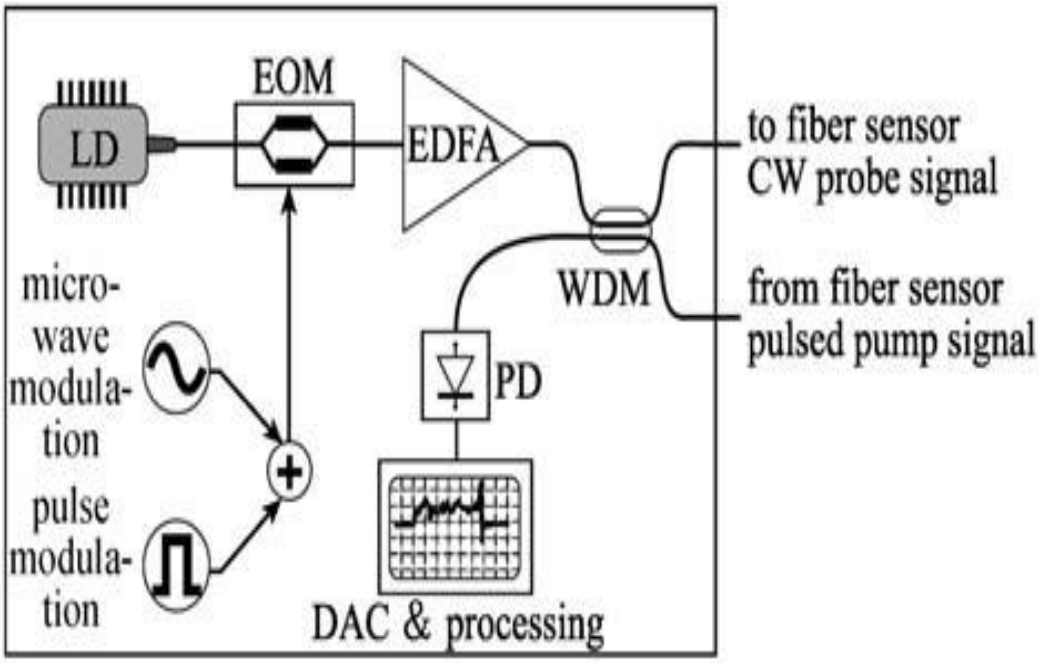

Figure2.7 BOTDA Setup [77]

CHAPTER 3

ANALYSIS OF BRILLOUIN FREQUENCY SHIFT & GAIN SPECTRUM

3.1 EDFA Power Analysis over Brillouin Gain Spectrum

For fiber optic configurations, mainly Erbium Dopes Fiber Amplifiers (EDFA) are used to amplify the optical waves. For BOTDA configurations, while the incident and probe waves are amplified, the scattered waves are also amplified. Using a classical BOTDA setup, the effects of EDFA power over Brillouin gain spectrum and Rayleigh power are observed. An EDFA power interval for optimum Brillouin readings for BOTDA configurations is proposed.

A classical BOTDA setup given in figure 3.1 is used for this experiment. The source is an adjustable TLS laser set at 1550.103nm with 0 dBm. The incident wave supplied by TLS laser is split into two with a 3 dB 1x2 coupler to supply for both pulse and pump waves. The usage of same laser source for both pulse and pump prevents optical frequency shifts that may happen in case of two laser different sources. One of the split wave is sent to Mach-Zender intensity modulator (MZM) to be modulated with a pulse generator. The pulse generator is set to provide an electrical pulse with repetition rate of 5 kHz and 200ns pulse duration. The modulated pulse signal is sent to Erbium doped fiber amplifier (EDFA1). The gain level of EDFA1 is not fixed since its effect on Brillouin peak frequency power level is to be observed. The amplified pulse wave is then sent to the 18.2km fiber under test (FUT) through a circulator. The other split incident wave is sent to another MZM to be modulated with an RF signal. RF generator is set to provide a 10 GHz sinusoidal signal. The modulated pump wave is sent to EDFA2 with fixed 101.21mA gain. The amplified pump wave is then sent to the other end of the FUT. Hence pump and pulse waves are sent in opposing directions to amplify the power transition between pulse and backscattered light. The backscattered pulse wave is sent to EDFA3 with fixed 20dB gain via circulator. The amplified backscattered wave is

then split into two with another coupler and respectively sent to high resolution optical spectrum analyzer (OSA) and to photodetector (PD). The electrical output of PD is sent to RF spectrum analyzer.

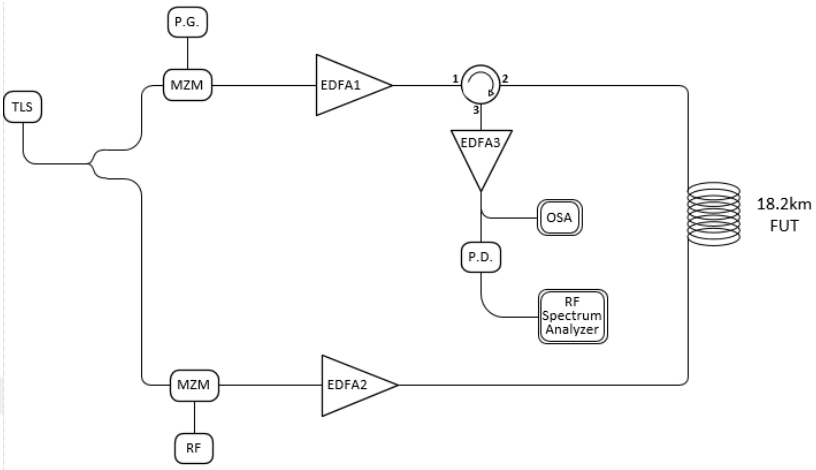

Figure3.1 Classical BOTDA Setup

The EDFA1 gain level is steadily incremented and the resulting RF Brillouin peak power level and optical Rayleigh and stimulated Brillouin scattering (SBS) power levels are observed. The resulting power graphs are shown in figures 3.2 and 3.3:

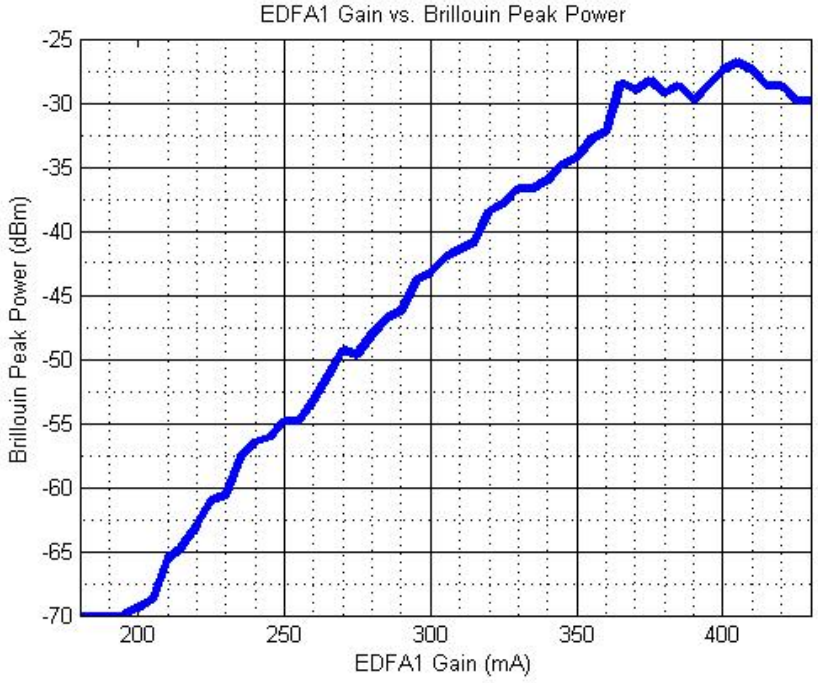

Figure3.2 Brillouin peak power vs EDFA1 gain

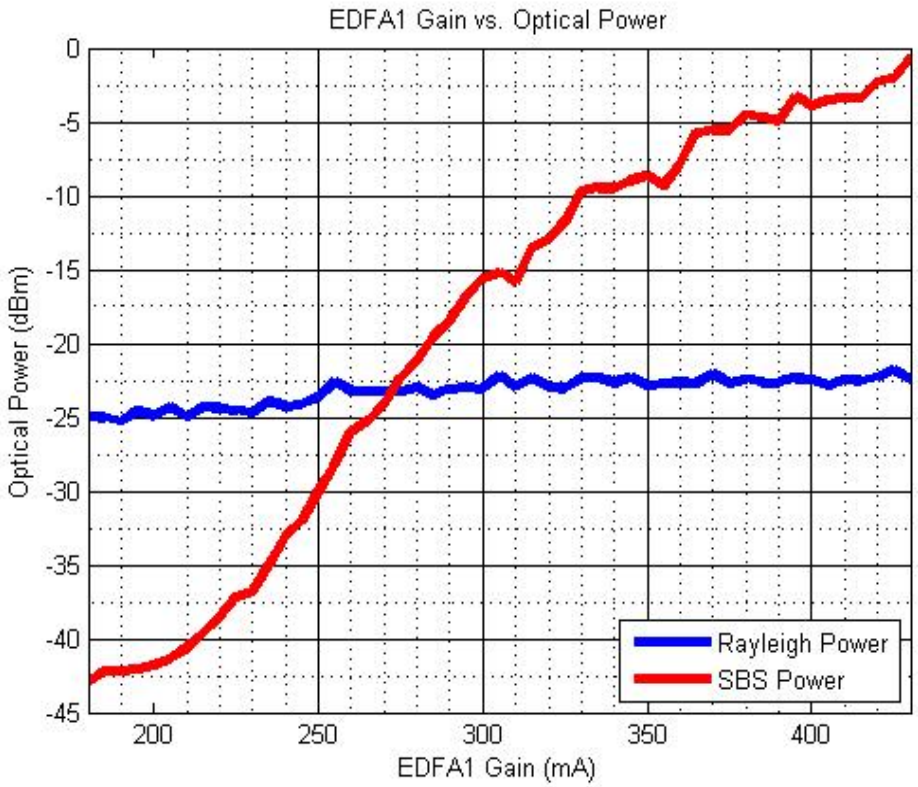

Figure3.3 Optical SBS and Rayleigh power vs EDFA1 gain

The EDFA1 gain level is steadily incremented and the resulting RF Brillouin peak power level and optical Rayleigh and stimulated Brillouin scattering (SBS) power levels are observed. The resulting power graphs are shown in figures 3.2 and 3.3:

3.2 Ambient Temperature and Fiber Length Analysis over Brillouin Frequency Shift

The experimental setup (BODTR) for observing the temperature dependence of Brillouin frequency shift on different length fiber cables is presented in Figure 3.4. An adjustable DFB laser source is used with settings tuned at; 1553 nm wavelength and 8.52 dBm power. The incident light wave from the source is first subjected to an Erbium Doped Fiber Amplifier with 8dBm gain. Then the amplified wave is sent to 95m single mode fiber under test (FUT) via a circulator. The other end of the fiber, attached with an FC/APC connector, is left unconnected.

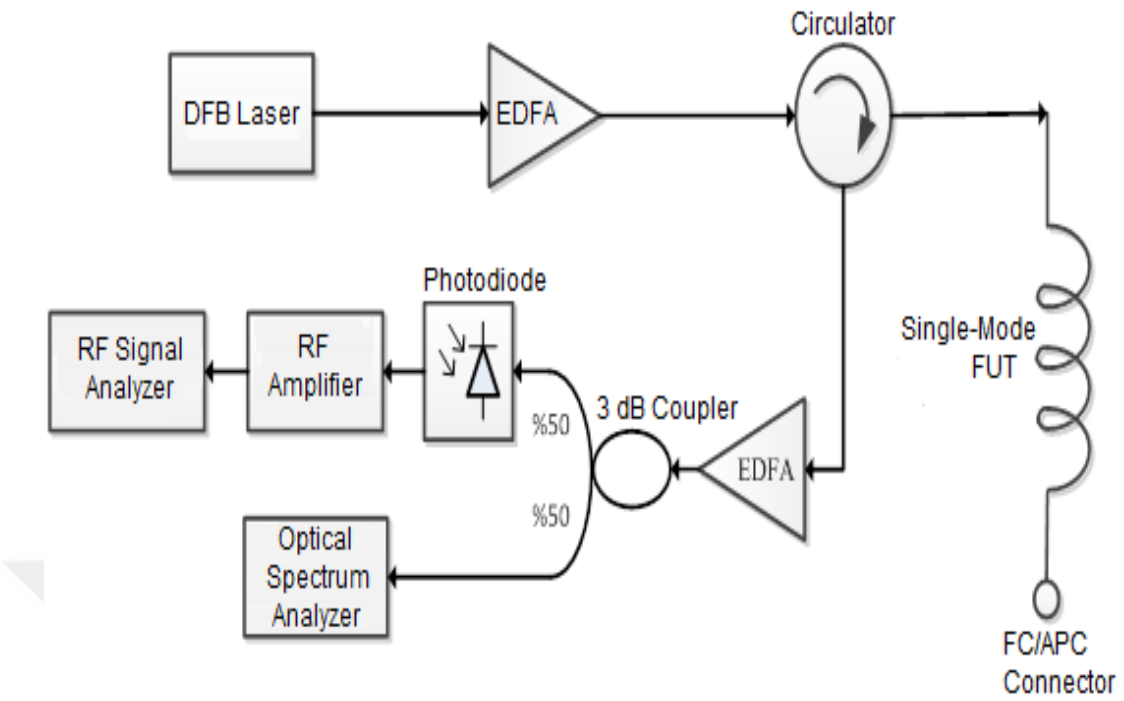

Figure3.4 Modern BOTDR test setup

The backscattered light, through the circulator, is sent to another EDFA which is fixed at 190mA gain. Then the amplified backscattered light is split into two with a 3dB 1x2 coupler and respectively sent to high resolution optical spectrum analyzer (OSA) and photodiode (PD). The electrical signal obtained from the photodiode is amplified with a Radio Frequency Amplifier (RFA) and sent to radio frequency spectrum analyzer (RFSA) to be analyzed.

First the FUT is subjected to 60ºC temperature with a furnace. After settling at this temperature, the Brillouin frequency shift of the reflected wave is observed with the high frequency signal analyzer. Then the temperature of the furnace is changed to 50ºC, 40ºC, 30ºC, 20ºC and 10ºC respectively and the Brillouin frequency shift at each temperature level is observed.

The frequency spectrum of Brillouin backscattered light on 95m FUT at temperature levels 30ºC and 20ºC are shown below;

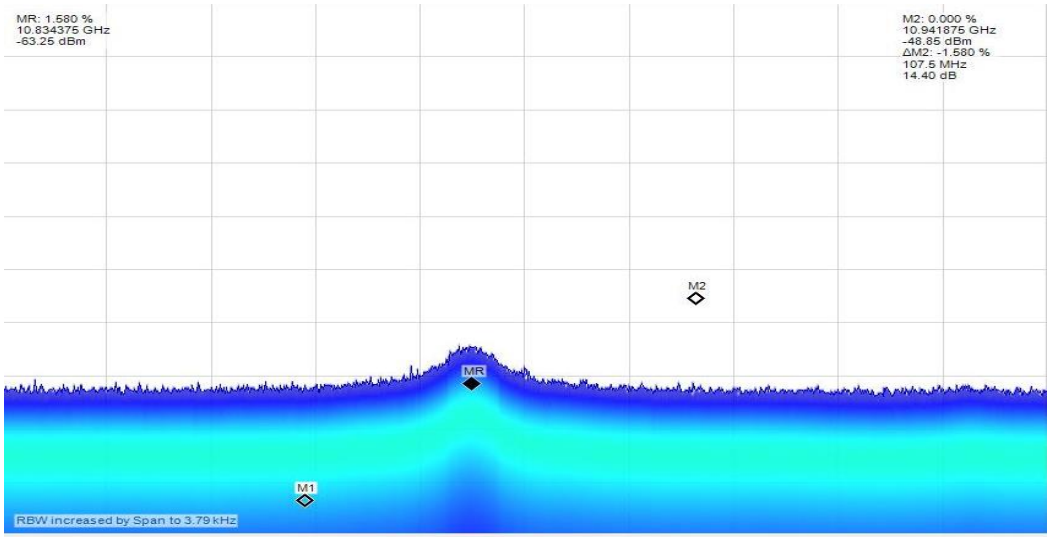

Figure3.5 Brillouin backscattering of 95m FUT at 30ºC (Peak frequency at 10.834375GHz)

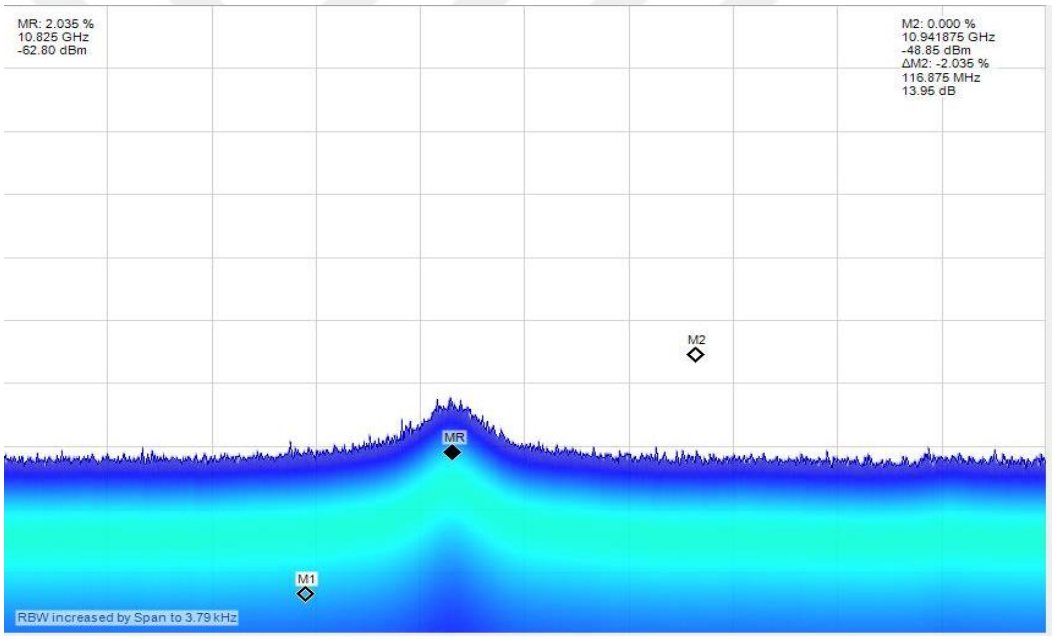

Figure3.6 Brillouin backscattering of 95m FUT at 20ºC (Peak frequency at 10.825GHz)

Using the peak frequency values at each temperature level, the Brillouin frequency shift vs temperature graph is given below;

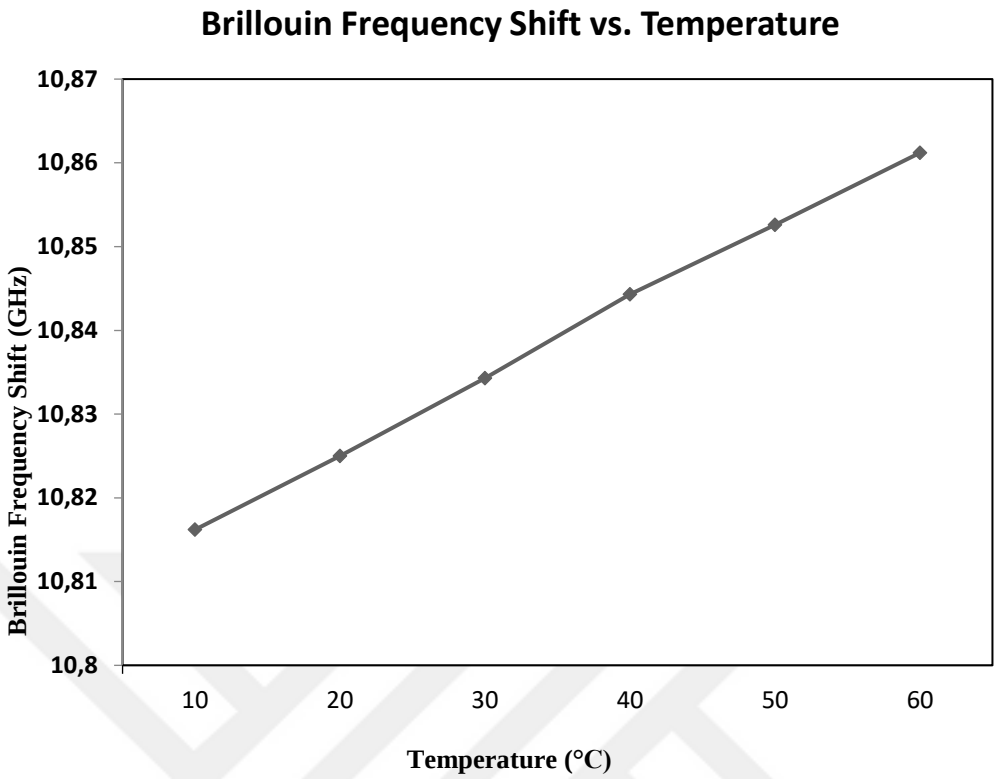

Figure3.7 The Brillouin frequency shift vs temperature of a single mode fiber

For the next step, using the same setup, temperature dependence of Brillouin frequency shift is observed for different FUT which are; 2.1 km SMF, 18km SMF, 200m shielded SMF buried 50cm deep into the ground and 40m SMF coiled around a drinking glass. These FUT are observed separately. The Brillouin frequency shift with respect to temperature of these fiber segments are shown as:

Table 3.1 Temperature vs Brillouin frequency shift on different fiber lengths

Fiber Length(m)	Temperature (°C)	Brillouin Frequency Shift (GHz)
2100	22	10,8400
18000	22	10,8610
200	10	10,8035
40	22	10,8330
40	95	10,8945

RF spectrum of Brillouin frequency shift for 2.1km SMF FUT is given,

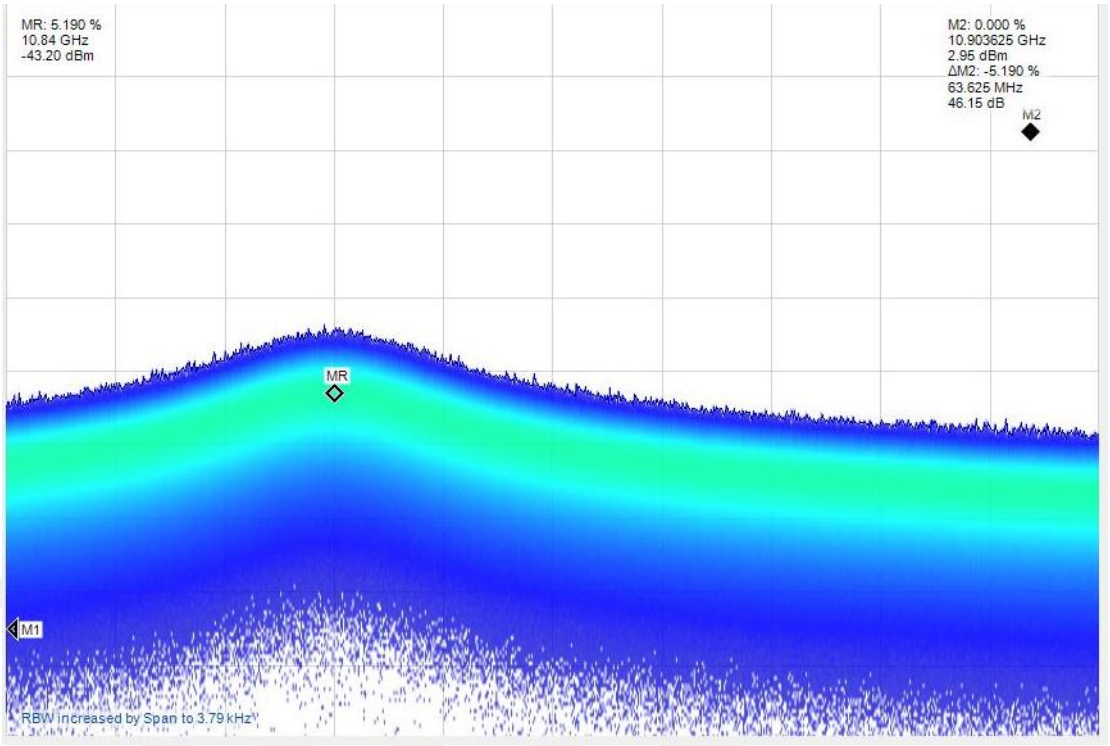

Figure3.8 Brillouin peak on 2.1km SMF FUT

RF spectrum of Brillouin frequency shift for 18km SMF FUT is given,

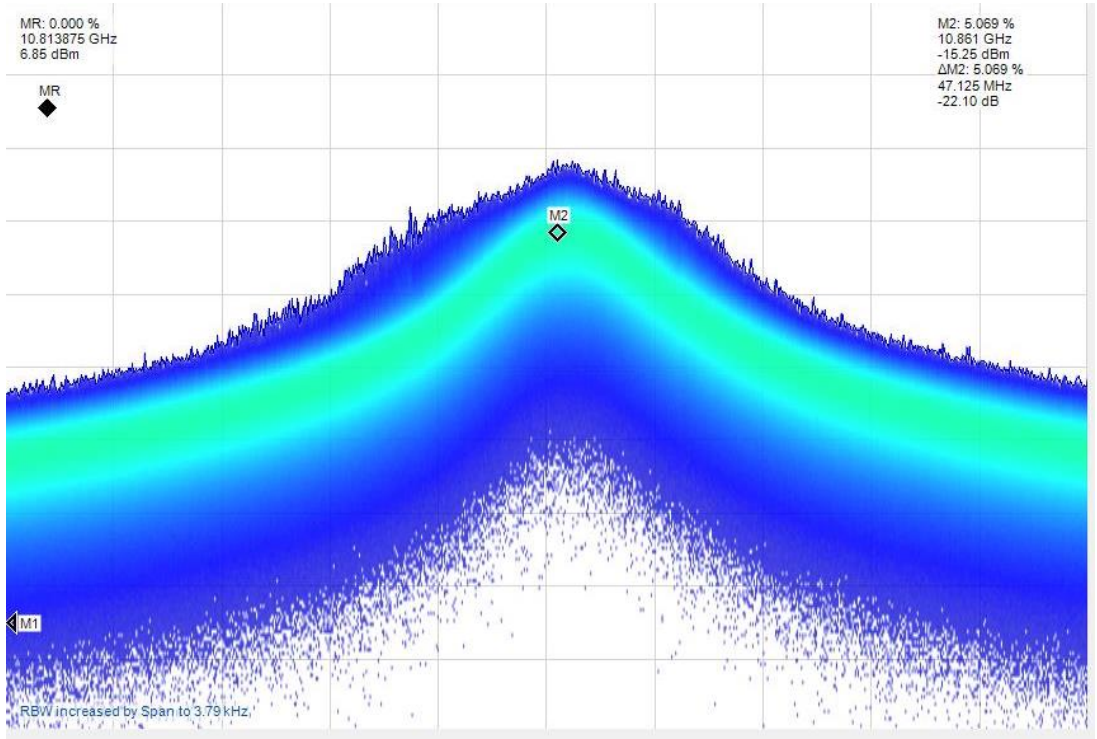

Figure3.9 Brillouin peak on 18km SMF FUT

Then 2.1km and 18 km fiber segments are both connected back to back to the test setup. The resulting RF spectrum of Brillouin frequency shift is given. These two different length and type segments produced two Brillouin frequency peak values.

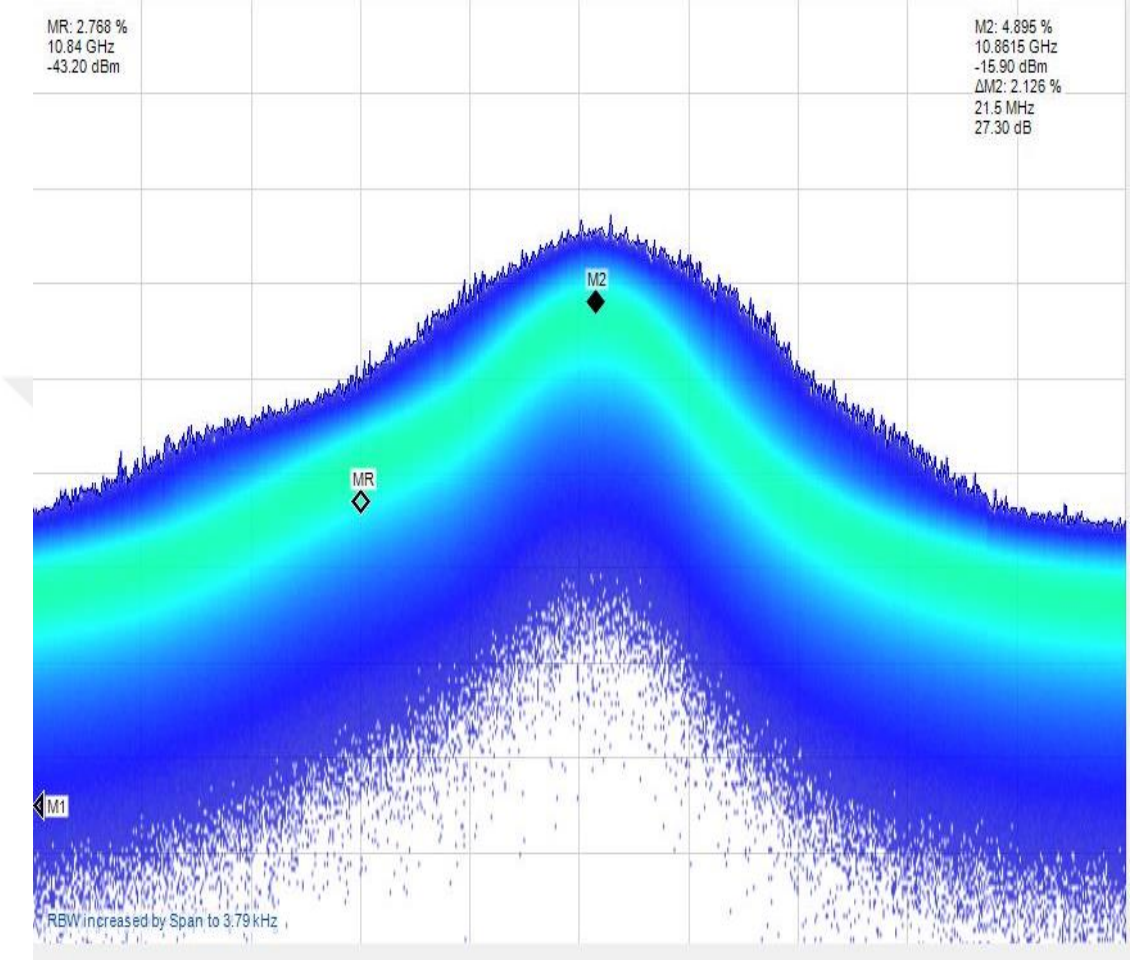

Figure3.10 Brillouin peak on 2.1km and 18km SMF FUT added back to back

Then 40m SMF coiled around glass is used as FUT. With this setup, experiment is conducted at both room temperature and with boiling water inside the glass. The respective Brillouin frequency shift RF spectrum and optical spectrum readings are shown in Figures 3.11, 3.12, 3.13 and 3.14:

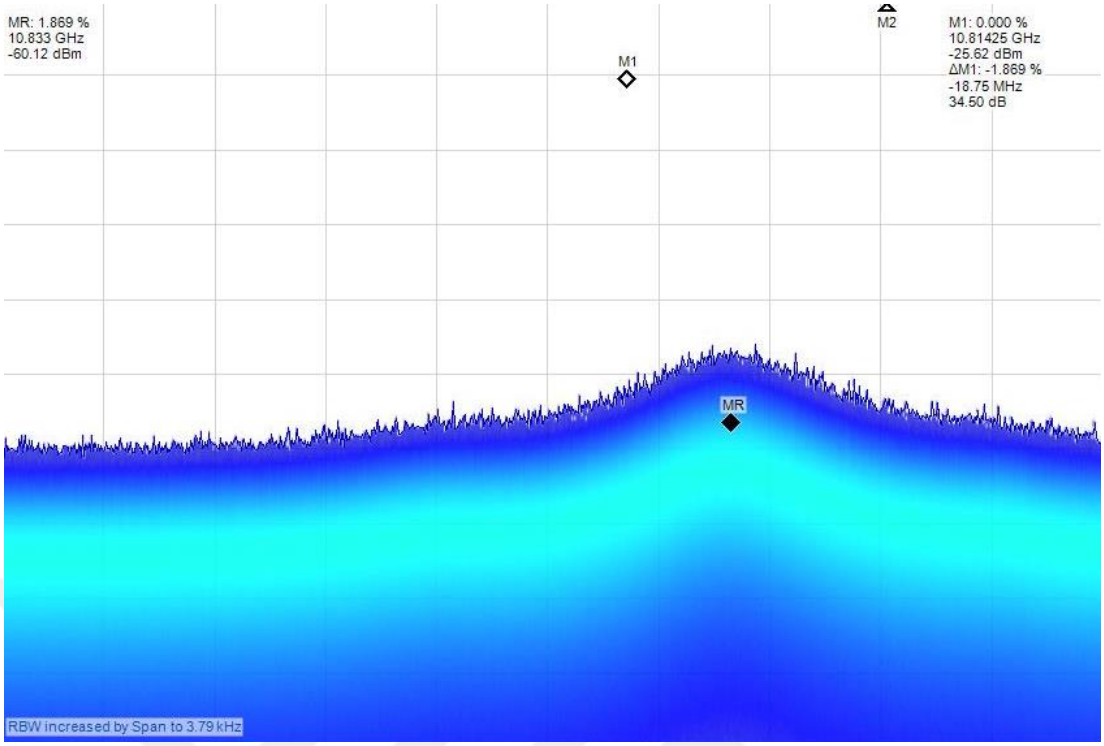

Figure3.11 Brillouin peak on 40m SMF FUT at room temperature

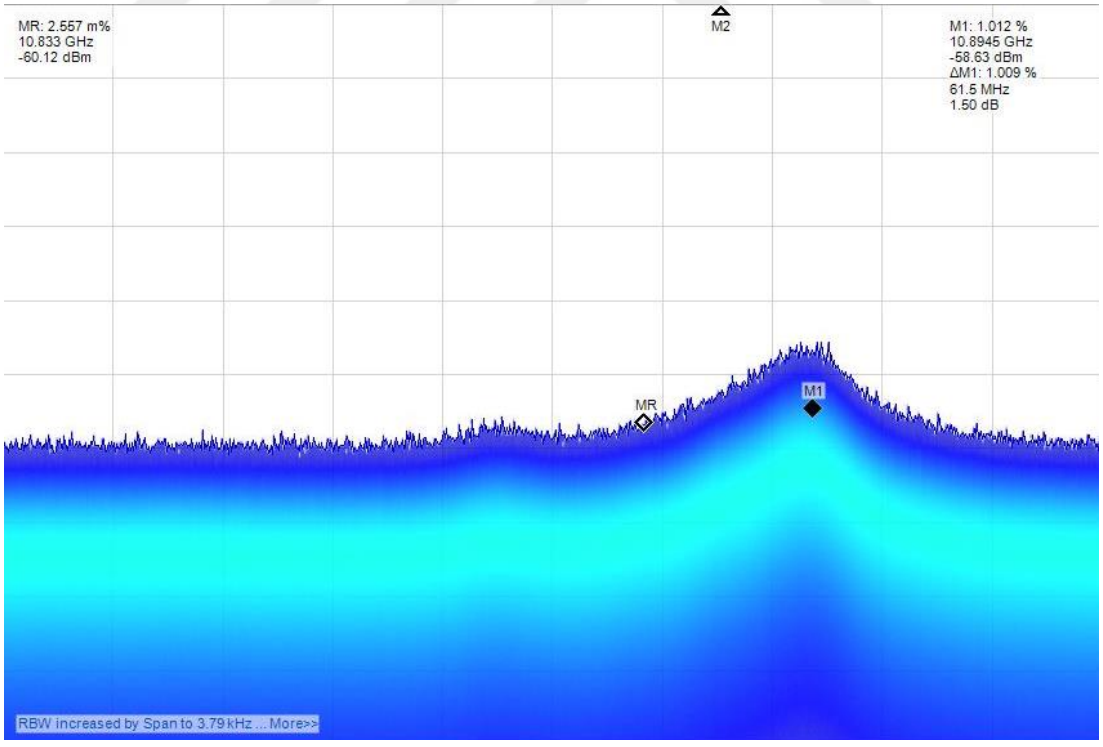

Figure3.12 Brillouin peak on 40m SMF FUT with boiling water

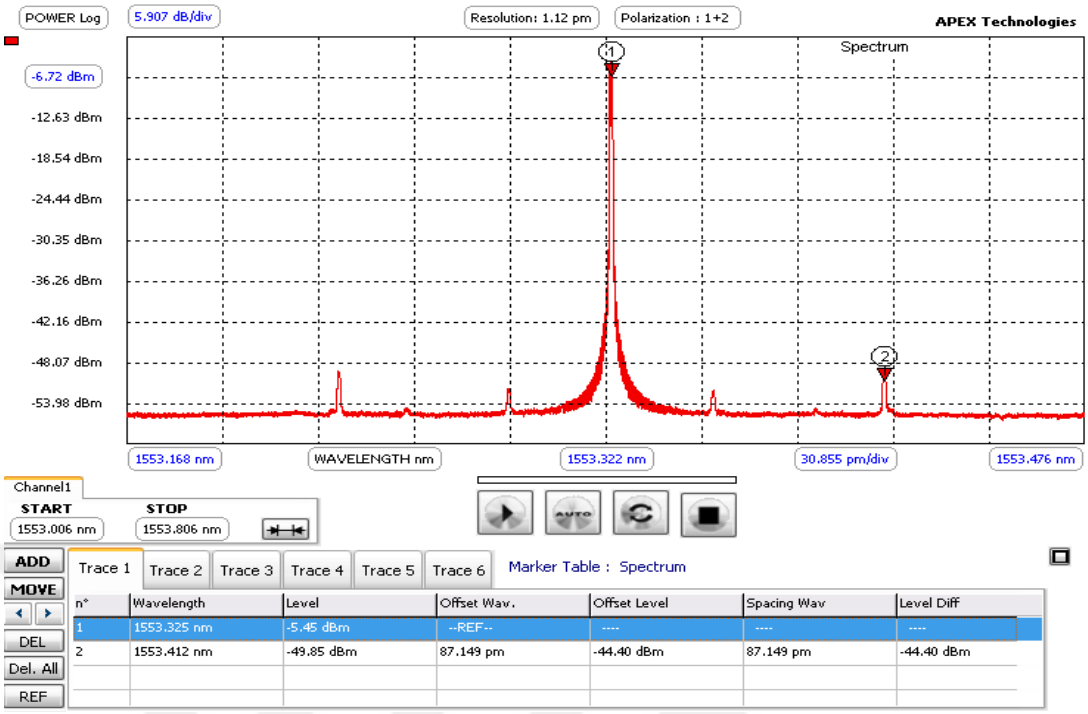

Figure3.13 OSA reading at room temperature (i.e. empty glass)

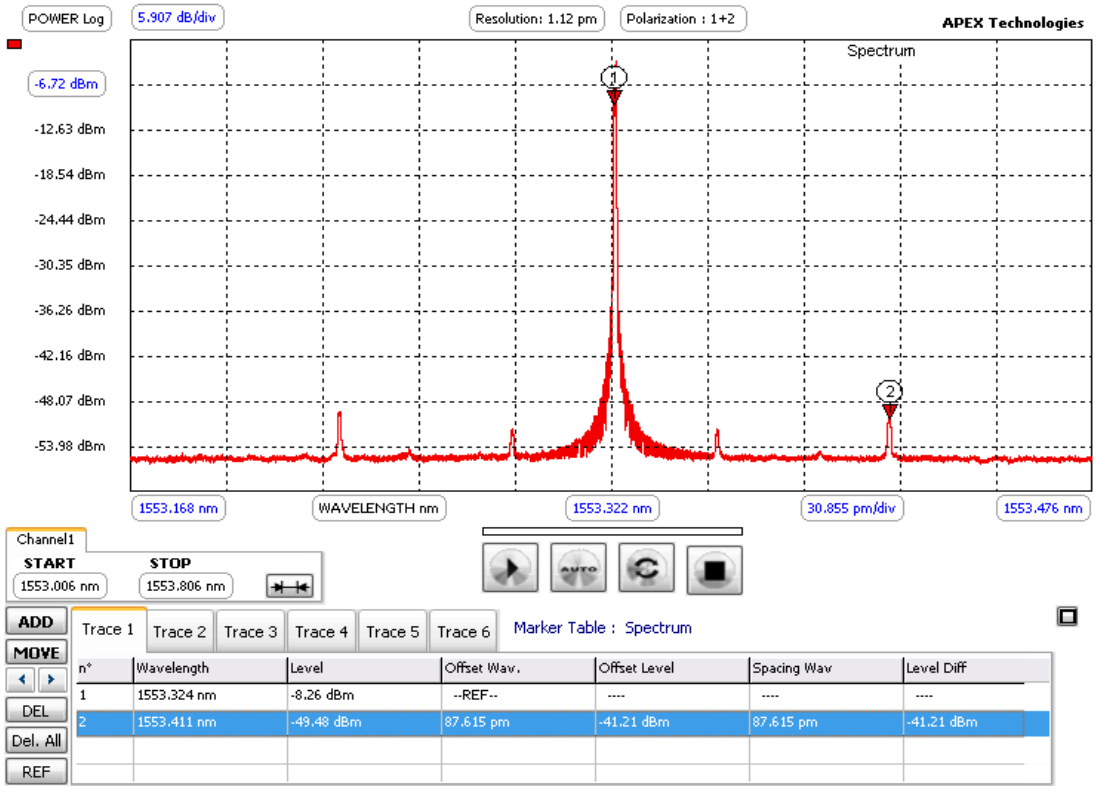

Figure3.14 OSA reading with boiling water inside glass

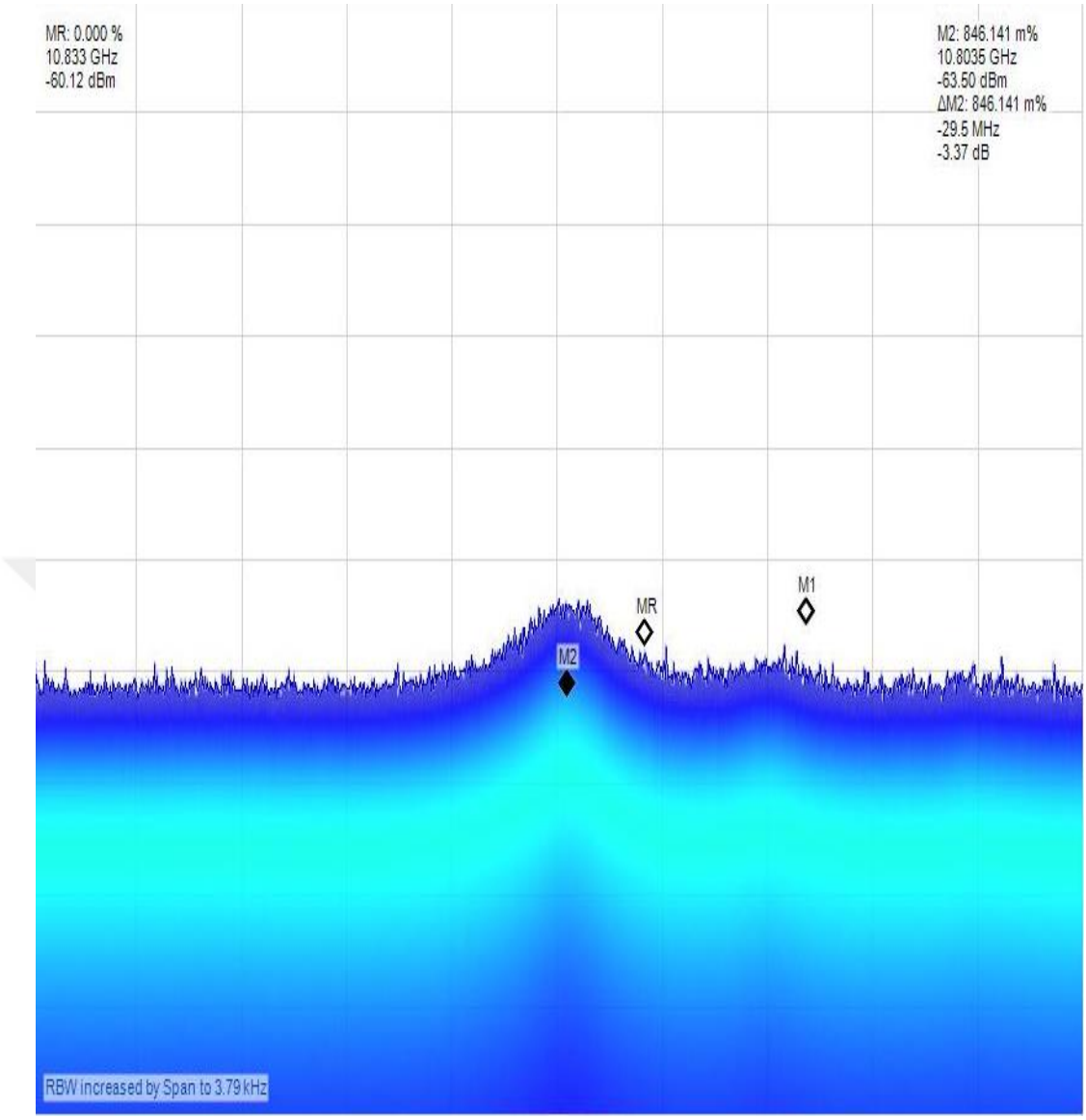

Figure3.15 Brillouin peak on 200m buried shielded SMF FUT

Then the buried 200m shielded SMF is connected to the test setup and the RF spectrum reading in Figure 3.15 is obtained.

The outside temperature during this experiment was measured at 18^{o}C and the underground temperature at 10^{o}C. The Brillouin frequency shift peak is measured at 10.8035GHz.

Finally, both the 40m coiled SMF and 200m buried shielded SMF are connected back to back to the test setup. The glass is filled with boiling water so as to observe

effects of both high and cold temperatures at the same time. The RF spectrum reading in Figure 3.16 is obtained:

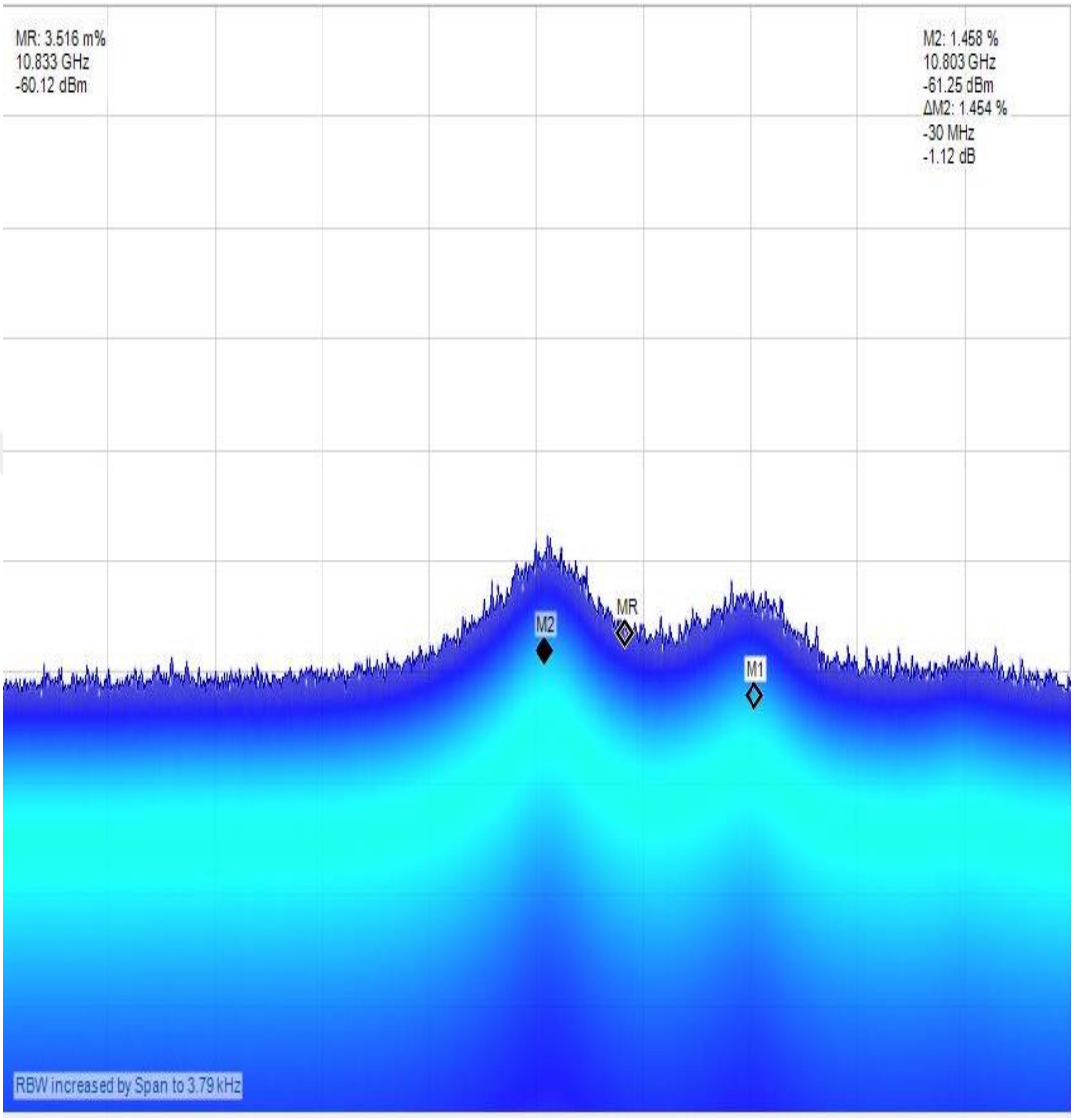

Figure3.16 Brillouin peak on 40m and 200m buried shielded SMF FUT connected

CHAPTER 4

CONCLUSION

The BOTDA EDFA power analysis shows that the Brillouin power has a linear dependence on source EDFA (i.e. EDFA1) and as the EDFA power increases, the Brillouin power also increased. This continued until EDFA power reached 360mA. From then on, the Brillouin power hits a plateau and stays same.

The Rayleigh power, however; is not affected by the EDFA power increase and stays the same throughout. The Brillouin optical power becomes higher than Rayleigh power around 270mA EDFA power.

For EDFA powers higher than 360mA, the cost of the system is increasing. For EDFA powers lower than 270mA, the Brillouin gain spectrum is very low. Hence in order to obtain a powerful enough Brillouin power, the EDFA power level should be set in between 270mA and 360mA.

Then the temperature effect on Brillouin frequency shift is observed with a BOTDR setup. As the temperature increases, the Brillouin frequency shift increases as well. The experimentally obtained Brillouin frequency shift vs temperature graph has a constant slope. Hence there is a direct relation between temperature and Brillouin Frequency shift. This is as expected as Brillouin frequency is primarily used as temperature sensor. The temperature affect can be observed much more closely using a higher temperature interval with smaller step increments. Also a higher resolution furnace for applying finer temperatures would help.

Then the fiber length effect on Brillouin frequency shift is observed using the same BOTDR setup. The longer the fiber length, the stronger Brillouin shift is obtained. This is due to the longer interaction of incident wave along the fiber. Additionally, the Brillouin frequency shift readings for BOTDR setup with low fiber lengths such as 40m and 90m are obtained. The acquired Brillouin readings are powerful enough to process.

Also, for the back to back added fiber cases, it is observed that there are two different Brillouin peaks at same temperatures. This is due to the fact that each fiber has a unique Brillouin frequency peak. Which means that, while splicing fibers for experimental purposes, it is strongly recommended to use same type and brand fibers. Otherwise, unwanted Brillouin frequency peaks may occur and mislead the experiment.

REFERENCES

[1] D. Hazarika, D.S. Pegu, *"Micro-controller based air pressure monitoring instrumentation system using optical fibers as sensor"*, Optical Fiber Technology Volume 19, Issue 2, Pages 83–87, 2013

[2] P. B. Buchade, *"Microcontroller Based Mobile Platform with Fiber Optic Sensors"*, Measurement Science and Technology, Volume 23, Number 3, 2013

[3] Alberto J. Palma, Javier L´opez-Gonz´alez, Luis J. Asensio, Maria Dolores Fern´andez-Ramos, Luis Fermin Capit´an-Vallvey, "Microcontroller-based portable instrument for stabilised optical oxygen sensor", Sensors and Actuators B: Chemical Volume 121, Issue 2, 20 February 2007, Pages 629–638, 2006

[4] Mahfoozur Rehman, Chew Eong Hoon, AmirAbu_Al Aish, Mohd Rizal Arshad, *"Remote measurement of liquid flow using turbine and fiber optic techniques"*, Mechanical Systems and Signal Processing Volume 25, Issue 5, Pages 1661–1666, 2011

[5] A. F. Omar, M. Z. MatJafri, *"Development of Optical Fiber Sensor for Water Quality Measurement",* AIP Conference Proceedings, Volume 1017, Issue 1, 10.1063/1.2940669, 2008

[6] N. C. Ryder, *"Microcontroller based data acquisition system for silicon photomultiplier Detectors"*, Topical Workshop on Electronics for Particle Physics, 2012

[7] Qiuhong Zhang and Qian Liu, *"Build intelligent home furnishing control system by microcontroller GSM and optical fiber sensor"*, Journal of Chemical & Pharmaceutical Research; Vol. 6 Issue 7, p1689, 2014

[8] Jiahong Zhang, Fushen Chen, Bao Sun, Chengxin Li, *"Wavelength tuning for LiNbO3 photonic sensor to have linear operation point"*, Microwave and Optical Technology Letters, Volume 55, Issue 10, Version of Record online, 2013

[9] Oleg Uzenkov, Peter Lee, D. Webb, "*An FPGA based Measurement System for a Fibre Bragg Grating (FBG) Strain Sensor*", Instrumentation and Measurement Technology Conference, Proceedings of the IEEE, 2006

[10] Graham Wild, Steven Hinckley, *"Distributed Optical Fibre Smart Sensors for Structural Health Monitoring: A Smart Transducer Interface Module"*, Intelligent Sensors, Sensor Networks and Information Processing (ISSNIP), 2009

[11] Altuğ, G. "*Fiber Optik Grating Sensörler*", Yüksek Lisans Tezi, Gazi Üniversitesi, 2007

[12] Qin, Z. *"Distributed Optical Fiber Vibration Sensor Based on Rayleigh Backscattering"*, Phd. Thesis, Ottawa University, 2013

[13] Karaman, L., Ünverdi, N.Ö., *"Fiber Bragg Izgara Tabanlı Optik Sensörün Analizi"*, IV. Ulusal Iletisim Teknolojileri Sempozyumu, Çukurova Üniversitesi, Adana, 1997

[14] Bao, X. Y., Chen, L., *"Recent Progress in Distributed Fiber Optic Sensors"*, Sensors, 12, 8601-8639, 2012

[15] Soto, M.A., Bolognini, G.; Pasquale, F.D.; Thévenaz, L. *"Simplex-coded BOTDA fiber sensor with 1 m spatial resolution over a 50 km range"*, Opt. Lett. 35:259-261, 2010

[16] Hao, H.; Li, W.; Linze, N.; Chen, L.; Bao, X. *"High resolution DPP-BOTDA over 50 km fiber using return to zero coded pulses"*, Opt. Lett. 35:1503-1505, 2010

[17] Barrios, F.R.; Lopez, S.M.; Sanz, A.C.; Corredera, P.; Castanon, J.D.A.; Thevenaz, L.; Herraez, M.G. *"Distributed Brillouin fiber sensor assisted by first-order Raman amplification"*, IEEE J. Lightw. Technol., 28:2162-2172, 2010

[18] Soto, M.A.; Bolognini, G.; Pasquale, F.D. *"Optimization of long-range BOTDA sensors with high resolution using first-order bi-directional Raman amplification"*, Opt. Express, 19,:4444-4457, 2011

[19] Jia, X.H.; Rao, Y.J.; Chen, L.; Zhang, C.; Ran, Z.L. *"Enhanced sensing performance in long distance Brillouin optical time-domain analyzer based on Raman amplification: theoretical and experimental investigation"*, J. Lightwave. Technol., 28:1624-1630, 2010

[20] Zornoza, A.; Pérez-Herrera, R.A.; Elosúa, C.; Diaz, S.; Bariain, C.; Loayssa, A.; *"Lopez-Amo, M. Long-range hybrid network with point and distributed Brillouin sensors using Raman amplification"*, Opt. Express, 18:9531-9541, 2010

[21] Sperber, T.; Eyal, A.; Tur, M.; Thevenaz, L. *"High spatial resolution distributed sensing in optical fibers by Brillouin gain-profile tracing"* Opt. Express, 18, 8671–8679, 2010

[22] Li, Y.; Chen, L.; Dong, Y.; Bao, X., *"A novel distributed Brillouin sensor based on optical differential parametric amplification"*, J. Lightwave Technol., 28:2621-2626, 2010

[23] Mafang, S.F., *"Brillouin Echoes for Advanced Distributed Sensing in Optical Fibres"*, Phd. Thesis, École Polytechnıque Fédérale De Lausanne, 2011

[24] Foaleng S. M., Tur M., Beugnot J-C. and Thévenaz L. *"High spatial and spectral resolutionlong-range sensing using Brillouin echoes"*, IEEE Journal Lightwave Technology, 28(20):2993-3003, 2010

[25] Andrew, M. *"Stimulated Brillouin Scattering in Single-Mode Optical Fiber"*, Phd. Thesis, University of Virginia, 1997

[26] M.N. Alahbabi, *"Distributed Optical Fiber Sensors Based on the Coherent Detection of Spontaneous Brillouin Scattering"*, Phd. Thesis, University of Southampton, Optoelectronic Research Centre, 2005

[27] Günday, A., *"Enerji Kablosunda Oluşan Sıcaklık ve Gerilmeleri Optik Fiberli Algılayıcılarla Algılama Benzetimleri"*, Yüksek Lisans Tezi, Uludağ Üniversitesi, 2007

[28] A. Günday, G. Yılmaz, S.E. Karlık, *"Optik Fiberli Dağınık Algılama Yöntemiyle Enerji Kablosunda Sıcaklık ve Gerginliğin Azalması"*, Uludağ Üniversitesi Mühendislik-Mimarlık Fakültesi Dergisi, Cilt 12, Sayı 2, 2007

[29] O Frazão, C Correia, J L Santos and J M Baptista, *"Raman fibre Bragg-grating laser sensor with cooperative Rayleigh scattering for strain–temperature measurement"*, Measurement Science and Technology, Volume 20, Number 4, 2009

[30] H.F.Martins, M. B. Marques and O. Frazão, *"Temperature-insensitive strain sensor based on four-wave mixing using Raman fiber Bragg grating laser sensor with cooperative Rayleigh scattering"*, Appl. Phys. B (2011) 104: 957. doi:10.1007/s00340-011-4516-1, 2011

[31] Yahei Koyamada, Mutsumi Imahama, Kenya Kubota, and Kazuo Hogari, *"Fiber-Optic Distributed Strain and Temperature Sensing With Very High Measurand Resolution Over Long Range Using Coherent OTDR"*, Journal of Lightwave Technology, Vol. 27, No. 9, May 1, 2009

[32] Mohamed N. Alahbabi, Yuh T. Cho, and Trevor P. Newson, "*150-km-range distributed temperature sensor based on coherent detection of spontaneous Brillouin backscatter and in-line Raman amplification*", Journal of the Optical Society of America B Vol. 22, Issue 6, pp. 1321-1324, 2005

[33] Yuelan Lu, Tao Zhu, Liang Chen, Xiaoyi Bao, *"Distributed Vibration Sensor Based on Coherent Detection of Phase-OTDR"*, Journal of Lightwave Technology Volume: 28, Issue: 22, 2010

[34] Dawn K. Gifford, Brian J. Soller, Matthew S. Wolfe, Mark E. Froggatt, *"Distributed Fiber-Optic Temperature Sensing using Rayleigh Backscatter"*, 31st European Conference on Optical Communications (ECOC 2005), page v3:511, 2005

[35] R. Posey, G. A. Johnson, S.T.Vohra, *"Strain sensing based on coherent Rayleigh scattering in an optical fibre"*, Electronics Letters Vol. 36 No. 20, 2000

[36] Alessandro Signorini, Tiziano Nannipieri, and Fabrizio Di Pasquale, *"High Performance Distributed Optical Sensors Based on Raman Scattering"*, OSA Technical Digest (online) Optical Society of America, paper FM4H.4, 2012

[37] Mostafa Ahangrani Farahani and Torsten Gogolla, *"Spontaneous Raman Scattering in Optical Fibers with Modulated Probe Light for Distributed Temperature Raman Remote Sensing"*, Journal of Lightwave Technology, Vol. 17, No. 8, 1999

[38] J. M. Bello and T. Vo-Dinh, *"Surface-Enhanced Raman Scattering Fiber-Optic Sensor"*, Applied Spectroscopy Vol. 44, Issue 1, pp. 63-69, 1990

[39] Hartog, A., *"A distributed temperature sensor based on liquid-core optical fibers"*, Journal of Lightwave Technology LT-1(3):498 – 509, 1983

[40] A. E. El-Taher, P. Harper, S. A. Babin, D. V. Churkin, E. V. Podivilov, J. D. Ania- Castanon, S. K. Turitsyn, *"Effect of Rayleigh-scattering distributed feedback on multiwavelength Raman fiber laser generation"*, Optics Letters Vol. 36, Issue 2, pp. 130-132, 2011

[41] Gabriele Bolognini, Jonghan Park, Marcelo A Soto, Namkyoo Park and Fabrizio Di Pasquale, *"Analysis of distributed temperature sensing based on Raman scattering using OTDR coding and discrete Raman amplification"*, Measurement Science and Technology, Volume 18, Number 10, 2007

[42] David L Stokes, Tuan Vo-Dinh, *"Development of an integrated single-fiber SERS sensor"*, Sensors and Actuators B: Chemical Volume 69, Issues 1–2, Pages 28–36, 2000

[43] Luca Palmieri, and Luca Schenato, *"Distributed Optical Fiber Sensing Based on Rayleigh Scattering"*, The Open Optics Journal, 2013, 7: 104-127, 2013

[44] Mark Froggatt, Dawn Gifford, Steven Kreger, Matthew Wolfe, and Brian Soller, *"Distributed Strain and Temperature Discrimination in Unaltered Polarization Maintaining Fiber"*, Optical Fiber Sensors OSA Technical Digest (CD) Optical Society of America, paper ThC5, 2016

[45] P. C. Wait, T. P. Newson, *"Landau Placzek ratio applied to distribute fibre sensing"*, Optics Communications Volume 122, Issues 4–6, Pages 141–146, 1996

[46] Ju Han Lee, You Min Chang, Young-Geun Han, Haeyang Chung, Sang Hyuck Kim, and Sang Bae Lee, *"Raman amplifier-based long-distance remote, strain and temperature sensing system using an erbium-doped fiber and a fiber Bragg grating"*, Optics Express Vol. 12, Issue 15, pp. 3515-3520, 2004

[47] Kazuo Hotate, *"Fiber distributed Brillouin sensing with optical correlation domain techniques"*, Optical Fiber Technology Volume 19, Issue 6, Part B, Pages 700–719, 2013

[48] A. Wosnioka, N. Nöthera, K. Krebbera, *"Distributed Fibre Optic Sensor System for Temperature and Strain Monitoring Based on Brillouin Optical-Fibre Frequency-Domain Analysis"*, Procedia Chemistry, Volume 1, Issue 1, Pages 397–400, Proceedings of the Eurosensors XXIII conference, 2009

[49] Hyungwoo Kwona, Suhwan Kim, Sehyuk Yeom, Byoungho Kang, Kyujin Kim, Taeheok Kim, Hangseok Jang, Jeehyun Kim, Shinwon Kang *"Analysis of nonlinear fitting methods for distributed measurement of temperature and strain over 36 km optical fiber based on spontaneous Brillouin backscattering"*, Optics Communications Volume 294, Pages 59–63, 2013

[50] A.H. Reshak, M. M. Shahimin, S.A.Z. Murad, S. Azizan *"Simulation of Brillouin and Rayleigh scattering in distributed fibre optic for temperature and strain sensing application"*, Sensors and Actuators A: Physical Volume 190, Pages 191–196, 2013

[51] Yosuke Mizuno, Zuyuan He, Kazuo Hotate, *"Distributed strain measurement using a tellurite glass fiber with Brillouin optical correlation-domain reflectometry"*, Optics Communications, Volume 283, Issue 11, Pages 2438–2441, 2010

[52] Yunqi Hao, Qing Ye, Zhengqing Pan, HaiwenCai, Ronghui Qu, Zhongmin Yang, *"Effects of modulated pulse format on spontaneous Brillouin scattering spectrum and BOTDR sensing system"*, Optics & Laser Technology Volume 46, March 2013, Pages 37–41, 2012

[53] Romeo Bernini, Aldo Minardo, Luigi Zeni, *"Distributed fiber-optic frequency-domain Brillouin sensing"*, Sensors and Actuators A: Physical Volumes 123–124, 23 September 2005, Pages 337–342 Eurosensors XVIII — The 18th European conference on Solid-State Transducers, 2004

[54] Y.D. Gong, *"Guideline for the design of a fiber optic distributed temperature and strain sensor"*, Optics Communications, Volume 272, Issue 1, Pages 227–237 2007

[55] V. Lecoeuche, D.J. Webb, C.N. Pannell, D.A. Jackson, *"25 km Brillouin based single-ended distributed fibre sensor for threshold detection of temperature or strain"*, Optics Communications, Volume 168, Issues 1–4, Pages 95–102, 1999

[56] P.C. Wait, K. De Souza, T.P. Newson, *"A theoretical based comparison of spontaneous Raman and Brillouin fibre optic distributed temperature sensors"*, Optics Communications, Volume 144, Issues 1–3, Pages 17–23, 1997

[57] Himansu Shekhar Pradhan, P.K. Sahu, *"150 km long distributed temperature sensor using phase modulated probe wave and optimization technique"*, Optik - International Journal for Light and Electron Optics, Volume 125, Issue 1, Pages 441–445, 2014

[58] Haroldo T. Hattori, Vitor M. Schneider, Osni Lisboa, Rogerio M. Cazo, *"A high nonlinearity elliptical fiber for applications in Raman and Brillouin sensors"*, Optics & Laser Technology, Volume 33, Issue 5, Pages 293–298, Optical Fibers and Applications, 2001

[59] Xue-Feng Zhao, LeLi, Qin Ba, Jin-Ping Ou, *"Scour monitoring system of subsea pipeline using distributed Brillouin optical sensors based on active thermometry"*, Optics & Laser Technology, Volume 44, Issue 7, Pages 2125–2129, 2012

[60] Lijuan Zhao, Yongqian Li, Zhiniu Xu, Zhi Yang, Anqiang Lü, *"On-line monitoring system of 110 kV submarine cable based"*, Sensors and Actuators A: Physical Volume 216, Pages 28–35, 2014

[61] V. Lecoeuche, P. Niay, M. Douay, P. Bernage, S. Randoux, J. Zemmouri, *"Bragg grating based Brillouin fibre laser"*, Optics Communications Volume 177, Issues 1–6, Pages 303–306, 2000

[62] R.A. Perez-Herrera, M. Lopez-Amo, *"Fiber optic sensor Networks"*, Optical Fiber Technology Volume 19, Issue 6, Part B, Pages 689–699, 2013

[63] II-Bum Kwon, Se-Jong Baik, Kiegon Im, Jae-Wang Yu, *"Development of fiber optic BOTDA sensor for intrusion detection",* Sensors and Actuators A: Physical Volume 101, Issues 1–2, Pages 77–84, 2002

[64] NAN Shiqing, GAO Qian *"Application of Distributed Optical Fiber Sensor Technology Based on BOTDR in Similar Model Test of Backfill Mining"*, Procedia Earth and Planetary Science Volume 2, Pages 34–39, The Second International Conference on Mining Engineering and Metallurgical Technology (MEMT), 2011

[65] Zhi Zhou, Minghua Huang, Jianping He, Genda Chen, Jinping Ou, *"Ice structure monitoring with an optical fiber sensing system"*, Cold Regions Science and Technology, Volume 61, Issue 1, Pages 1–5, 2009

[66] Femi Tanimola, David Hill, *"Distributed fiber optic sensors for pipeline protection"*, Journal of Natural Gas Science and Engineering, Volume 1, Issues 4–5, Pages 134–143, 2009

[67] Si Zhi Yan, Lee Sheng Chyan, *"Performance enhancement of BOTDR fiber optic sensor for oil and gas pipeline monitoring"*, Optical Fiber Technology, Volume 16, Issue 2, Pages 100–109, 2010

[68] Yingchun Ding, Junbo Gao, Shi Shen, *"Controlling waveform of light pulse with light in optical fibers"*, Optik - International Journal for Light and Electron Optics, Volume 125, Issue 16, Pages 4505–4507, 2014

[69] Murat Yücel, Murat Yücel, A. Erkam Gündüz, H. Haldun Göktaş, Nail Ferhat Öztürk, *"Using single-mode fiber as temperature sensor"*, Signal Processing and Communication Application Conference (SIU), 24th, 2016

[70] Murat Yücel, Nail Ferhat Öztürk, Murat Yücel, H. Haldun Göktaş, A. Erkam Gündüz, *"Design of a Fiber Bragg Grating based temperature sensor"*, Signal Processing and Communication Application Conference (SIU), 24th, 2016

[71] Z Fang, K Chin, R Qu, H Cai(auth.), K Chang(eds.)., *"Fundamentals of Optical Fiber Sensors"*, Wiley, Pages 292–294, 2012,

[72] Meyer-Arendt, Jurgen R., *"Introduction to Classical and Modern Optics"*, 2nd Ed, Prentice-Hall, 1984. 3rd Ed, 1989, 4th Ed,

[73] R Nave., *"Mie Scattering"*, Hyperphysics.phy-astr.gsu.edu, 2016. Available: http://hyperphysics.phy-astr.gsu.edu/hbase/atmos/blusky.html, Accessed: 5 Nov 2016

[74] Edouard Brainis, *"Spontaneous Nonlinear Scattering Processes in Silica Optical Fibers"*, Recent Progress in Optical Fiber Research, Pages: 26-44, 2012

[75] S. P. Singh, R. Gangwar, N. Singh, *"Nonlinear Scattering Effects in Optical Fibers"*, Progress In Electromagnetics Research, PIER 74, 379–405, 2007

[76] Xin Feng, Jing Zhou, Changsen Sun, Xiaotan Zhang, Farhad Ansari, *"Theoretical and Experimental Investigations into Crack Detection with BOTDR-Distributed Fiber Optic Sensors"*, Journal of Engineering Mechanics, Vol.139, Pages: 1797-1807, 2013

[77] Luc Thevenaz, *"Brillouin distributed time-domain sensing in optical fibers: state of the art and perspectives"*, Optics Letters Vol. 36, Issue 2, pp. 130-132, 2010

RESUME

Abdullah Erkam GÜNDÜZ was born in Samsun, in 1987. He received the BSc degree in Electrical-Electronics Engineering from İhsan Doğramacı Bilkent University. He is currently working as reserach assistant in the Department of Electrical and Electronics Engineering in Yıldırım Beyazıt University. He is still a graduate student in the Department of Electrical and Electronics Engineering of Graduate School of Natural Sciences of Yıldırım Beyazıt University. His research interests are fiber optic sensors and digital signal processing.

2016 ANKARA	**Department of Electronics and Communication Engineering**	**Abdullah Erkam GÜNDÜZ**	